I give permission for public access to my thesis and for copying to be done at the discretion of the archives' librarian and/or the College library.

_____ _____

Signature Date

Respiratory Effects of hTau Overexpression in *Drosophila melanogaster* Astrocytes

by

Vanessa Renee Farkas

A paper presented to the
Faculty of Mount Holyoke College in
Partial Fulfillment of the Requirements for
the Degree of Bachelors of Arts with
Honor

Program in Neuroscience and Behavior
South Hadley, MA 01075
May 2025

This paper was prepared
under the direction of
Professor Kenneth J. Colodner
for eighth credits.

To my wife: for you the world

ACKNOWLEDGMENTS

To Blaire, I am so serious when I say that none of this would be possible without you. And, I know your feminist brain would logically agree that you should be named first in this section. If I am a neuron, then you would be my astrocyte. I am forever grateful for the work you did to help me complete this project. I know you say your labor is simply reciprocal from when I helped you with your thesis, but I still feel indebted for every action you have done for me to get me to where I am. No words can ever encapsulate the aid every hug and kiss gave, nor could I ever plot them all in a graph. As we move through this world of uncertainty, there really is no one I'd rather be with than you. To be loved is to be changed, and your love bleeds into all my actions.

To Mom, Dad, and Robyn, thank you for accepting me for the person I am and allowing me to follow my passion. It is a blessing to have a family that shows you what it is like to experience unconditional love. I know that no matter what I do I will always make you proud, but I hope despite the bar being on the ground, that you feel satisfied with how your daughter turned out. Thank you so much for all of your continued support and love.

To Lara and Mike, it has been so wonderful to become a part of your family. I cannot thank you enough for all the support you have given me over the years. Despite me not being your daughter, you have welcomed me in like one. I am proud to call you a part of my family, and I look forward to visiting with you in Spain!

To Mister Fig, although you will never be able to read this, I still want to give my thanks to you. It was always easier to write with you sleeping next to me, even though you snore really loud. You helped me remember to eat, sleep, and take breaks to play. You were my practice audience for all my presentations, and although you could never give critical feedback, your presence still helped. Without you, this would have been so much harder. Your joyful attitude towards life inspires me to keep moving forward. I will always try my best to provide you with the best life I can. While I can never know what your happiest memories are, I hope that I am in at least some

of them. I will personally find a way to reverse the aging process in cats just to extend my time on Earth with you.

To my fellow seniors – Becks, Kamlyn, Birdy, Sky, Katie, and Danyah – I am so happy that I got to complete this project with the support and companionship of you all. Not to sound too much like the power of friendship, but it is amazing how we wrote four theses, and completed three independent projects (I think that has to be some kind of MHC record, right?). All of you are going to do amazing things and I am so excited to see what you all accomplish. If anyone gives you crap, remember you are so much more amazing and deserve so much more than that (and also you have my number).

To Aitana and Stella, when Ken asked me if I wanted mentees, I was so unsure of myself and my ability to pass on my knowledge. You two were the best students I could ever ask for. I valued your curiosity and passion for learning science. At the time when I first met you, I was undergoing health struggles that made doing my work very difficult. Both of you made the chore of showing up a delight. You both inspired me to consider pursuing teaching in the future, and I look forward to seeing you thrive at whatever you put your mind to.

To my fellow CLAN members, thank you for making our lab not only a supportive and welcoming place, but a fun place. As I think about continuing my scientific career, I worry that I may have already gotten to experience the cream of the crop in terms of people to work with. This will be difficult to say goodbye to, and I know you all will continue to be amazing and do awesome work.

To my honors committee Jared and Gary, thank you for all of your support and help on this project. Thank you for being friendly faces in the halls of Clapp and Reese. I know that I can be stubborn about my work, but I am so grateful for all of your wisdom, advice, and input you gave me on this project despite it all.

To Janelle, if I was stuck on a deserted island, I hope you would be on it as well. I appreciate your careful planning and working hard to accommodate me during my multiple surgeries. If I

was in charge of giving out awards for employee of the month at Mount Holyoke, you would be the recipient every single month. I have never met a more hardworking and dedicated person to their craft. I am so grateful for all that you have done to support me in this process.

To Ken, it is difficult to not make this the longest, sappiest thank you ever. In the fall, I told Rae Nishi a secret; that I was not ready to leave. And, this spring, I still feel the same. She told me that there are other labs that do similar research and other labs that work with fruit flies. That may be true, but your shoes in my mind will be difficult and likely impossible to fill. I came into your lab knowing next to nothing about neuroscience, struggling to understand my 100 level courses, and slogging through day to day life trying to learn how to live. I honestly do not know what you saw in me freshman year, but I am so glad you let me into your research lab. You ignited a passion in me for science that I did not know I had, and I can only hope I can find a way to repay all of the hours you put into making me the scientist I am today.

TABLE OF CONTENTS

LIST OF FIGURES

Page

ABSTRACT

Difficulty breathing is a common symptom reported among patients with Alzheimer's disease. A number of neurodegenerative diseases including Alzheimer's involve insoluble aggregates of the microtubule-associated protein, tau. Due to the association between neurodegeneration and changes in respiration, there is more to uncover about these respiratory processes within the brain and how the protein tau affects respiration at the cellular level. This project will use the *Drosophila melanogaster* model animal, which possesses a tubular respiratory system called the trachea. Previous observation has shown that astrocytes associate closely with the trachea. In addition, it has been shown that mammalian astrocytes directly control cerebral capillary blood flow. This project aims to determine the potential for astrocytes to modulate the brain's respiratory process within the fruit fly by observing changes to respiration rate when human Tau (hTau) is overexpressed in astrocytes. This project's goal is to further the knowledge of how tauopathies like Alzheimer's and other neurodegenerative diseases affect the metabolic processes at the cellular level.

INTRODUCTION

Chapter 1: Respiration and Glia

1.1 Respiration and the Tracheal System

Respiration is an important process that occurs in every living organism, including insects. The primary goal of this process is to intake oxygen (O_2) and release carbon dioxide (CO_2). The oxygen taken in goes through a cellular process known as the Krebs cycle or the citric acid cycle (TCA), which uses oxygen to produce adenosine triphosphate (ATP), which is used to fuel other cellular functions. CO_2 is a by-product of the TCA cycle and CO_2 output is directly correlated to O_2 input (Fig. 1). This means that for every oxygen molecule taken in through the body, an equivalent amount of CO_2 is produced.

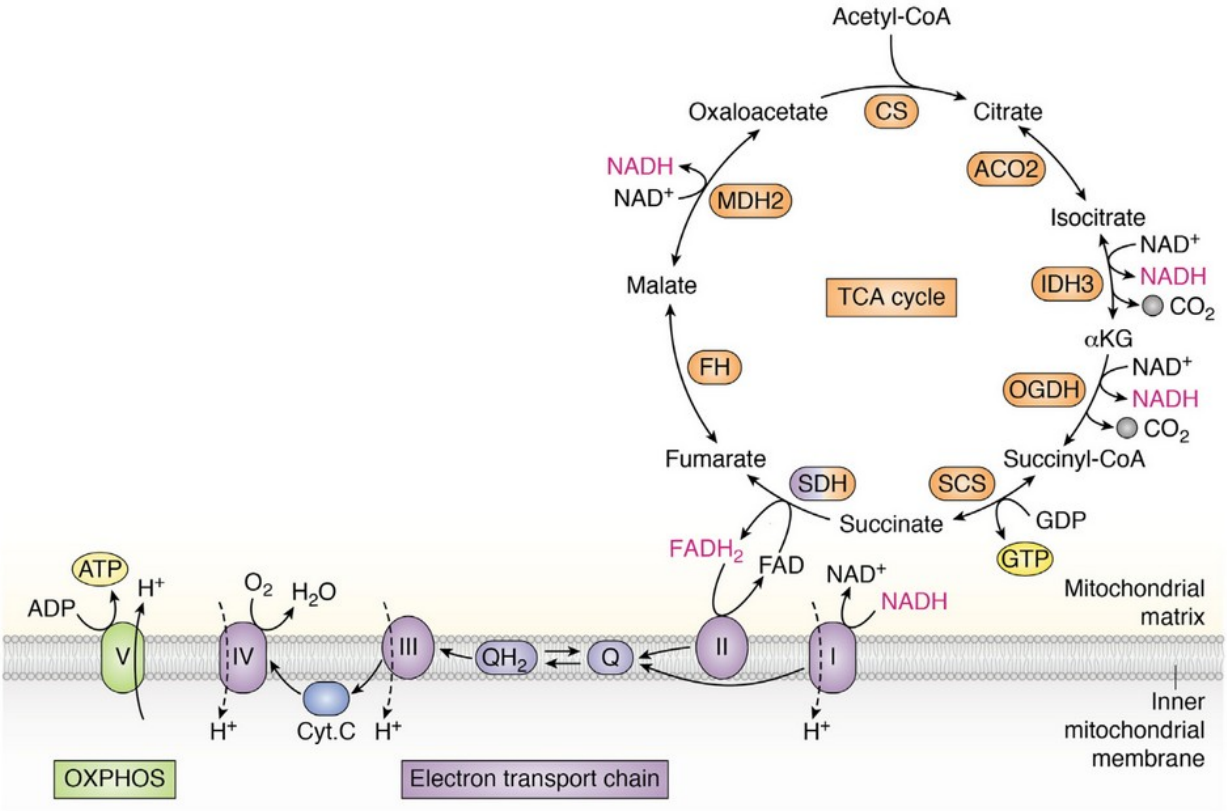

Figure 1. Cellular respiration via the citric acid cycle uses oxygen to produce ATP. Citrate is oxidized to form two CO_2 molecules and one ATP. Oxygen is required for the production of ATP as it acts as a terminal electron acceptor for the Electron Transport Chain (ETC). This process is referred to as oxidative phosphorylation (OXYPHOS) and is necessary for the production of ATP. Figure adapted from Arnold and Finely, 2023.

The brain is reliant on timely oxygen delivery, as a readily available source of ATP is crucial for synaptic activity to occur. It is estimated that 70% of ATP produced in the brain is used to fuel the sodium-potassium pump, a critical transport protein that maintains extracellular and intracellular concentrations of sodium and potassium (Voet & Voet, 2011). Synaptic transmission would be improbable without the work of the sodium potassium pump, and the sodium potassium pump would not function without systems of oxygen delivery.

Humans and many other organisms have respiratory systems that utilize a set of lungs to pump in/out oxygen and carbon dioxide. Deoxygenated blood is carried by the pulmonary arteries to the lungs to deposit CO_2 waste and obtain O_2 (Ehrlich et al., 2016). Fruit flies and other insects lack a set of lungs and instead rely on a respiratory system of tubes and air sacs

referred to as the trachea. The trachea spans the entire body of the fruit fly including inside the brain (Wigglesworth, 1939) (Fig. 2a). Oxygen enters the trachea through one of the many openings across the fly's body called spiracles (Fig. 2d). The spiracles also play an important role in preventing dehydration by reducing water loss through these openings (Lehmann, 2001).

During the early development of the fruit fly, trachea grows inward starting from these spiracles. The cuticle develops in a crinkle-cut shape to provide stability for the structure to prevent it from collapsing in on itself (Fig. 2b). The epithelial cells line the entirety of the trachea walls, with the thickest cells closest to the spiracles (Wigglesworth, 1939). The trachea contains different layers of these epithelial cells to help determine what can pass through its walls and what cannot. Oxygen, carbon dioxide, and water vapor are able to diffuse through and be absorbed by the epicuticle barrier, whereas more complex particles cannot pass through (Moussian, 2010). Within the human respiratory system, complex particles can be exhaled or removed by coughing (Morawska & Buonanno, 2021).

Respiratory systems differ in structure and shape for mammals and insects, but share the same purpose of oxygen delivery. Without systems to deliver oxygen to cells, all cellular functions would be halted, and life would cease to be. When respiratory systems are compromised, less ATP is produced and thus cellular functions become strained. It is important to understand how these systems function, but also what cells could contribute to maximizing energy production from respiration.

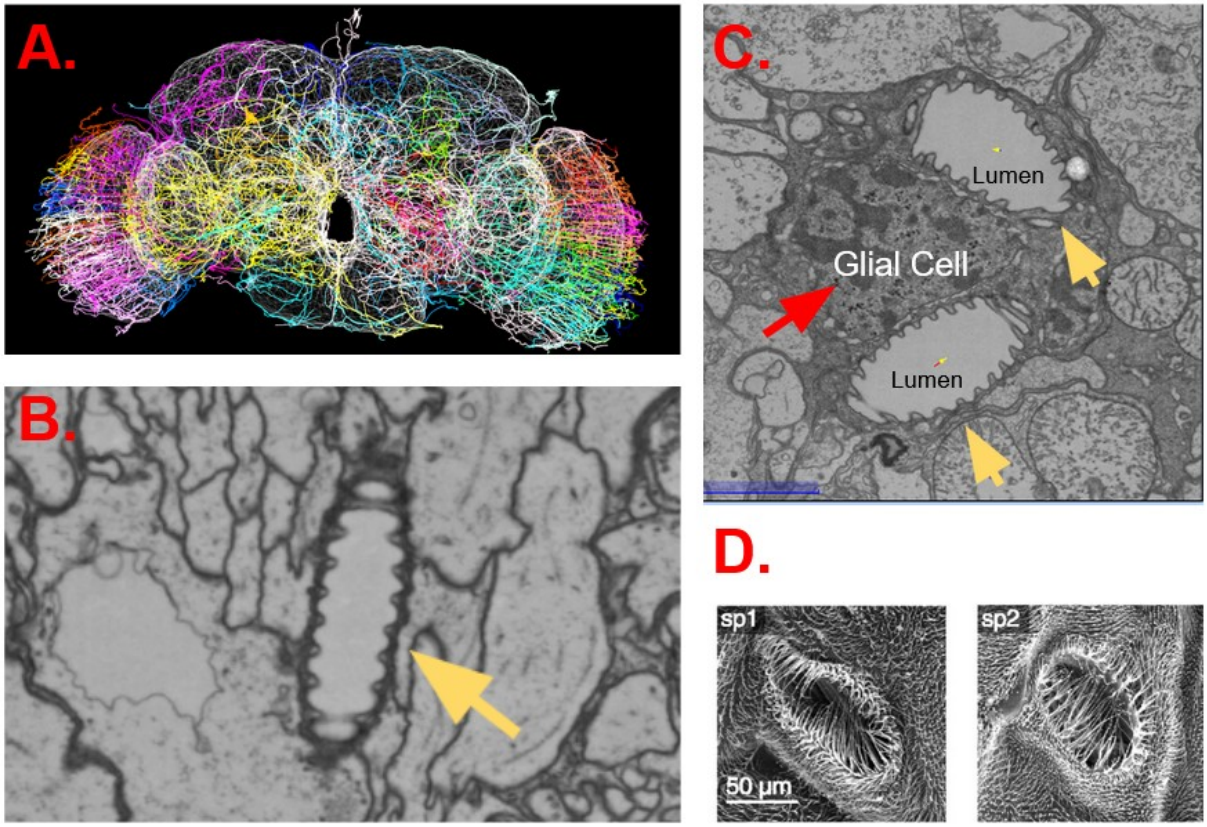

Figure 2. *Drosophila melanogaster* cerebral tracheal system. (A) Tracheal tubing spans the entire fruit fly body including the brain. (B) Yellow arrow pointing to cerebral trachea in TEM micrograph. (C) TEM micrograph depicting glial cells (red arrow) surrounding cerebral trachea (yellow arrows). (D) SEM micrographs of *Drosophila virilis* spiracles . Figure 2a, b & c are adapted from Colodner Lab, unpublished data. Figure 2d is adapted from Lehmann, 2001.

1.2 Glial Cells

Glial cells, defined as non-neuronal cells within the nervous system, were first described as “neuroglia” by Rudolf Virchow in 1856 (Kettenmann & Verkhratsky, 2008). They were first thought to be cells that held the neurons in the nervous system together, hence the word “glia” coming from the Ancient Greek word for glue, gloía (γλοία). This idea of merely being structural support cells has been refuted through many different scientific discoveries related to their unique cellular functionality, necessity for proper nervous system development, and symbiotic relationship with neurons (Fan & Agid, 2018). The term “glial cell", in vertebrates, encompasses

several different subtypes of glia including astrocytes, oligodendrocytes, and microglia. Each different subcategory of glia has its own function and localization within the nervous system, but all glial cells are necessary for proper brain structure and function. Glia are present in every bilaterian nervous system, although the subtype and function of glia differ across species (Sheloukhova & Watanabe, 2024).

1.3 Glial Cells in Humans

Glial cells are present in both the human central nervous system (CNS) and peripheral nervous system (PNS). Glia in the human CNS consists of astrocytes, oligodendrocytes, and microglia, among others (Fig. 3). Schwann cells and satellite glia are found only in the PNS. Both oligodendrocytes and Schwann cells are types of ensheathing glia, meaning these cells are responsible for myelinating the axons of neurons (Salzer, 2015). Microglia are self-renewing, immune system defense cells specific to the CNS (Nayak et al., 2014). Their primary role is to respond to injury within the brain. Satellite glia wrap around sensory neurons in the sensory ganglia and support these neurons metabolically (Hanani, 2005).

Astrocytes are the most common glial cells found throughout the CNS with many vital functions. Astrocyte-secreted thrombospondins (TSP1 and TSP2) are necessary for inducing synaptogenesis. In TSP1 and TSP2 knock-out mice, the amount of intracortical synapses are significantly reduced (Christopherson et al., 2005). Beyond synapse formation, calcium, an ion needed for neurotransmitter release at the synapse, is collected and released by astrocytes for neuronal use (Santello & Volterra, 2008). Along with calcium, potassium is collected and released by astrocytes. Astrocytes can also alter neuronal activity by recycling, releasing, and uptaking neurotransmitters at the synapse (Anderson and Swanson, 2000). When synapses are abundant in an area near an astrocyte, astrocytes will release potassium to increase the extracellular potassium concentration, which will then allow for more (or stronger) synapses to occur (Walz, 2000). In addition to ion release, astrocytes also perform ion clean up, in which excess synaptic ions are absorbed by astrocytes, as well as neurotransmitters and ATP (Santello & Volterra, 2008). The astrocytic collection and transfer of potassium from different synapses is energetically taxing, as astrocytes use both Kir4.1 channels and the sodium potassium pump to collect potassium. This results in astrocytes using almost as much ATP as a neuron during the potassium exchange process (Barros, 2022).

Astrocytes have a unique star-shape that allows them to reach up to two million synapses at one time (Fields et al., 2014). This is a valuable adaptation given that astrocytes are a necessity for neuron survival. The relationship between astrocytes and neurons extends beyond the synapse, as astrocytes have been found to metabolically support neurons. *In silico* models of experimentally induced cerebral hypoxia show that astrocytes supply neurons with additional metabolic support molecules such as lactate and glucose (Cakir et al., 2007). This allows for the neuron to attempt to continue its normal cellular processes under oxidative stress. Under the astrocytic hypoxia condition, astrocytes are quick to enact alternative anaerobic respiration (such as glycolic respiration). Due to the high metabolic demand of both the astrocyte and the neuron, proximity to a source of oxygen is important for both of these cells to function healthily.

All glial cells broadly are thought to have a neuro-protective purpose to them. However, this symbiotic relationship comes with a cost, as disruption of glial processes can result in neuronal death or dysfunction. For instance, neurons have a limited capacity to counteract oxidative damage from reactive oxygen species (ROS), whereas astrocytes and microglia are more resistant due to glycolic respiration (Rose et al., 2017). Neurodegeneration is observed when glial-specific glycolysis is genetically knocked down, but neuron-specific glycolysis is dispensable (Logan, 2017; Miller et al., 2012; Volkenhoff et al., 2015). Moreover, diseases that damage glial function directly damage neuronal function as well, due to the symbiosis between these cell types.

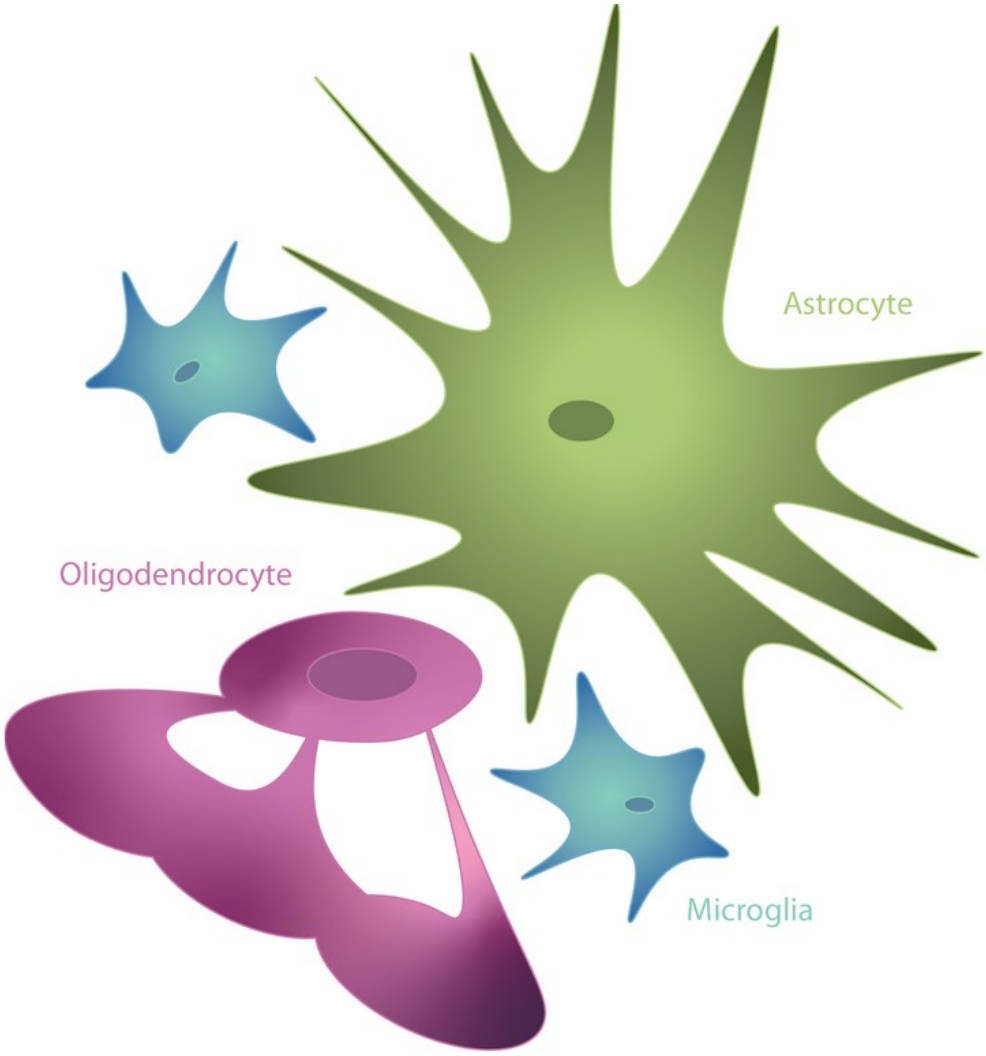

Figure 3. Representative image of mammalian CNS glial subtypes. Microglia (blue) are immune system defense cells. Oligodendrocytes (pink) are myelinating glia. Astrocytes (green) metabolic support neurons and assist with synaptic transmission and neurotransmitter uptake.

1.4 Astrocytic Vascular and Respiratory Control in Rodents

In mammals broadly, astrocytes act as a translational intermediary between the vascular system and neurons, as astrocytes associate closely with cerebral blood vessels (Fig. 4) (Fields & Stevens-Graham, 2002; Takano et al., 2006; Zonta et al., 2003). In rat cortical slices, neural activity directly increases calcium concentrations in astrocytes which also increases vasodilation (Takano et al., 2006; Zonta et al., 2003). This shows that astrocytes are involved in controlling blood flow within the brain as a response to meet the metabolic needs of neural activity.

Astrocytes in the ventral surface of the medulla oblongata (VS) of rats have been shown to directly control breathing (Gourine et al., 2010). VS astrocytes were found to be pH sensitive and respond to a decreased pH within the blood by increasing intracellular concentrations of calcium and increasing amounts of ATP released. This ATP release then activates chemoreceptor neurons, which results in the physiological response of increased breathing (Gourine et al., 2010). This proves that astrocytes play an active role in directly altering breathing patterns based on pH levels within the blood. These experiments show that astrocytes modulate the breathing process within rats.

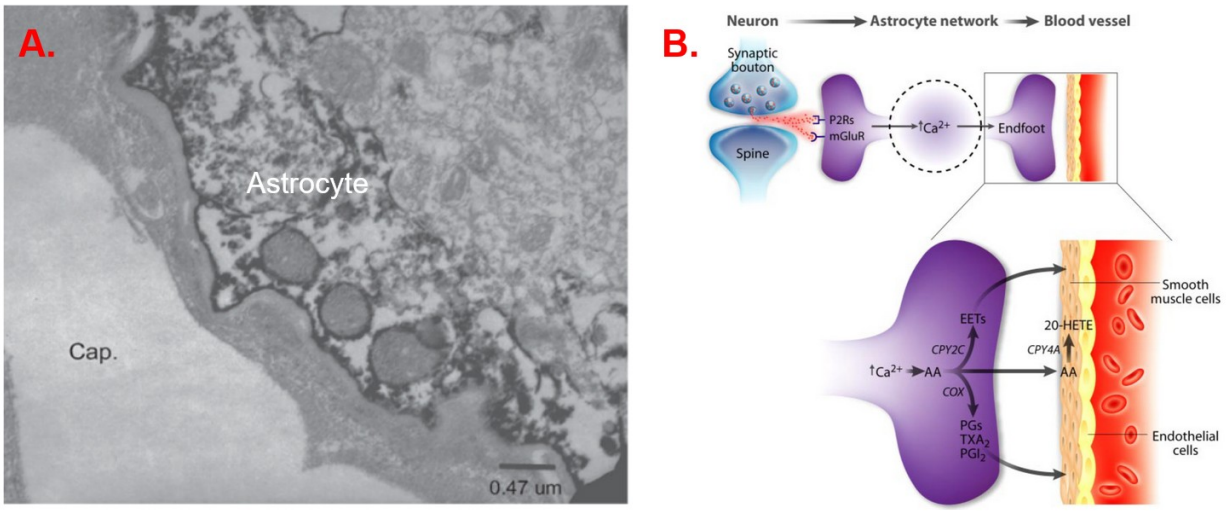

Figure 4. Mammalian astrocytes can constrict or dilate arteriole smooth muscle. Astrocytes can be found adjacent to capillaries (A). Glutamate release from neurons results in calcium increase in astrocytes. This calcium increase results in the production of metabolites with astrocytes such as arachidonic acid (constricts arteriole smooth muscle) or epoxyeicosatrienoic acids (dilates arteriole smooth muscle) (B). The dilation or constriction of arteriole smooth muscle alters blood flow and is directly coupled to neuronal activity. Figure 3a is adapted from Oberheim et al., 2009. Figure 3b is adapted from Haydon and Carmignoto, 2006.

1.5 Glial Cells in *Drosophila melanogaster*

Drosophila melanogaster possesses glial cells with similar functions to mammalian glia (Freeman, 2015). There are multiple subtypes of glia in *Drosophila* that include perineurial glia, subperineurial glia, cortex glia, ensheathing glia, and astrocytes (Fig. 5) (Perenau et al., 2005). Perineurial glia are found on the outermost layer of the central nervous system and exist to act as both a chemical and physical barrier to protect the central nervous system. Beneath the perineurial glia is the subperineurial glia. The role of the subperineurial glia is to form the blood brain barrier (BBB) (Auld et al., 1995) (Perenau et al., 2005). Both perineurial and

subperineurial glia do not associate closely with neurons, as their primary purpose is to protect and gate what can come in and out of the nervous system.

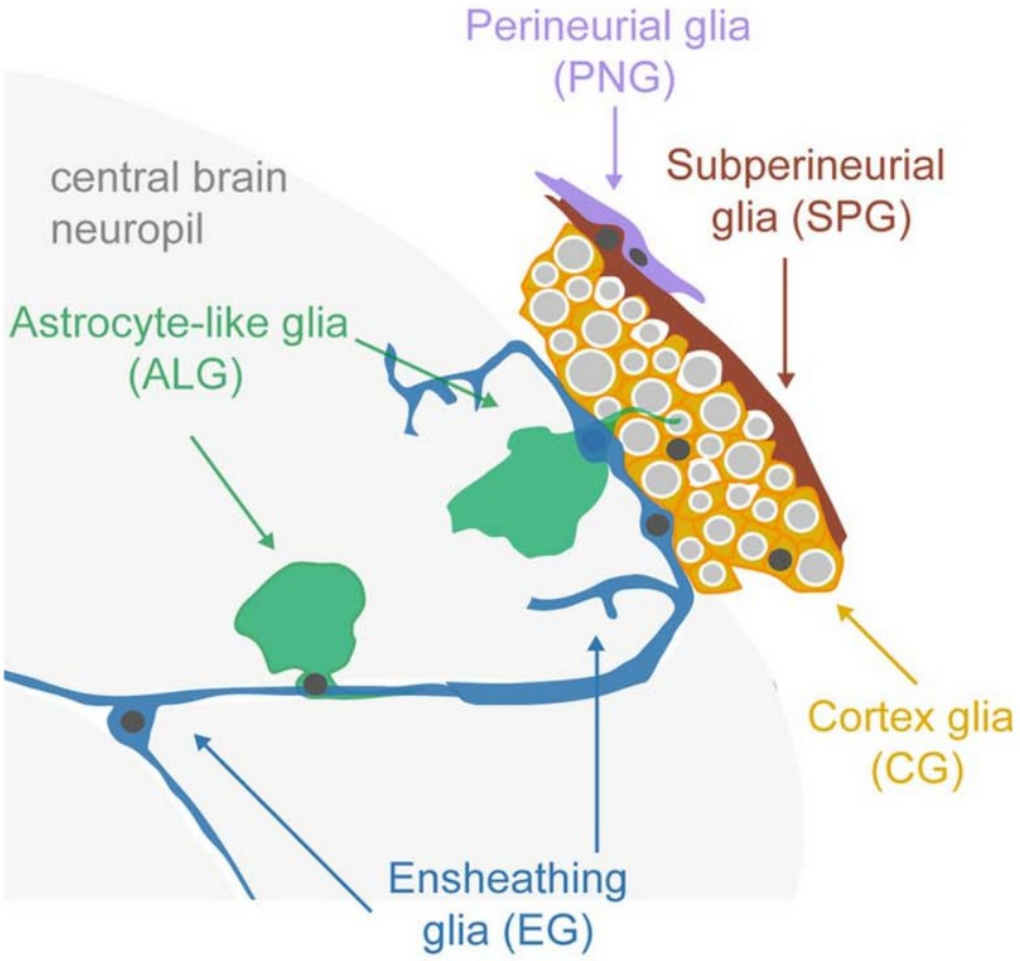

Figure 5. Representative image of *Drosophila melanogaster* CNS glial subtypes. Perineurial glial (purple) and subperineurial glial (red) act as protective barriers of the CNS. Cortex glial (yellow) ensheathes neuronal cell bodies in the cortex. Ensheathing glial (blue) help to form and protect axonal fiber tracts in the neuropil. Astrocytes (green) in flies are similar to mammalian astrocytes and are sometimes referred to as astrocyte-like glia. Figure adapted from Kremer et al., 2017

There are three main types of glia that interact with neurons in *Drosophila*: astrocytes, cortex glia, and ensheathing glia. Cortex glia are found in the cortex and completely ensheath neuronal cell bodies, providing protection and support (Perenau et al., 2005). Ensheathing glia surround the neuropil and divide boundaries between cortex and neuropil (Hartenstein, 2011) (Perenau et al., 2010). These glial cells ensheath and protect fiber tracts within the neuropil, and

are necessary for proper formation of the fiber tracts (Leiserson et al., 2000). Astrocytes are present in both *Drosophila* and humans. *Drosophila* astrocytes are morphologically similar and share many functions with astrocytes found in humans and other mammals (Freeman, 2015; Stork et al., 2012).

There are many similarities between mammalian astrocytes and fruit fly astrocytes. Both modulate synaptic transmission, metabolically support neurons, and can take up excess neurotransmitters (Freeman & Doherty, 2006). Mammalian astrocytes and Drosophila astrocytes share the same shape and tiling patterns across the CNS (Stork et al., 2014; Yildirim et al., 2019). There are many *Drosophila* astrocyte homologs for genes found in mammalian astrocytes (Huang et al., 2015). *Drosophila* astrocytes are similar to mammalian astrocytes across morphological, developmental, functional, and genetic categories (Freeman & Doherty, 2006). *Drosophila* and mammalian nervous systems anatomically differ, but share a cell type. This validates the use of *Drosophila* as a model animal to study astrocytes.

1.6 Glial-Tracheal Interactions

While the trachea serves an important purpose as a source of oxygen to produce ATP for both glial cells and neurons, it also has possible interactions with glial cells. One study determined that glial cells are crucial for proper trachea development, as when all glial cells are genetically knocked out, the trachea massively overgrows into the neuropil (Pereanu et al., 2007). The neuropil is a dense area classified by axon and dendrites of neurons, but not the cell bodies of those neurons. Given the high metabolic demand of synapses, having trachea grow appropriately next to these spaces is necessary.

One glial cell of interest in its relationship to the trachea is astrocytes. The relationship (or possible interaction) between trachea and astrocytes is speculated upon due to the fact that fruit fly astrocytes are adjacent to trachea structures in electron micrographs of the fly brain (Fig. 2c) (Freeman, 2015). It was found that astrocytes contain activity independent calcium microdomain channels that drive tracheal filopodia growth during development. Trachea filopodia that grow into these calcium microdomains exhibit a retraction behavior seconds after contact with the calcium microdomain (Ma & Freeman, 2020). These calcium microdomain channels are mediated by the Transient Receptor Protein (TRP) channel, TrpML. When TrpML is genetically knocked out or knocked down, calcium microdomains are no longer present, which

leads to tracheal overgrowth. These astrocytic calcium microdomains also closely align with the trachea, showing that they are necessary for proper development of this tube system within the brain (Ma & Freeman, 2020).

Astrocytes are found to be adjacent to respiratory structures across species. A widely accepted framework in biology is that structure corresponds to function (Herman et al., 2021). This means that the way in which a cell is arranged and located informs possible functions a cell might have. Since astrocytic capillary control and astrocytic respiratory control are functions proven in rats, by association of cell type and cell location and given the similarity astrocytes have across species, there is a substantial background to suggest that astrocytes modulate the respiratory process within the brain of fruit flies.

Chapter 2: Tau and Tauopathies

2.1 Tau as a Protein

The microtubule-associated protein tau was first identified and isolated in 1975 (Weingarten et al., 1975). Tau is found most abundantly in the axons of neurons, as its primary function is to organize and stabilize microtubules (Trojanowski et al., 1989). Neurons need to dynamically change the size and shape of their axons to meet the needs of synaptic activity.

One way that tau is able to stabilize microtubules is by phosphorylation. Under healthy tau phosphorylation, the addition of a phosphate group disconnects tau from the microtubule (Johnson and Stoothoff, 2004). However, when tau becomes hyperphosphorylated, it detaches completely from the microtubule and can form what is referred to as a neurofibrillary tangle (NFT) or aggregations of hyperphosphorylated tau (Fig. 6).

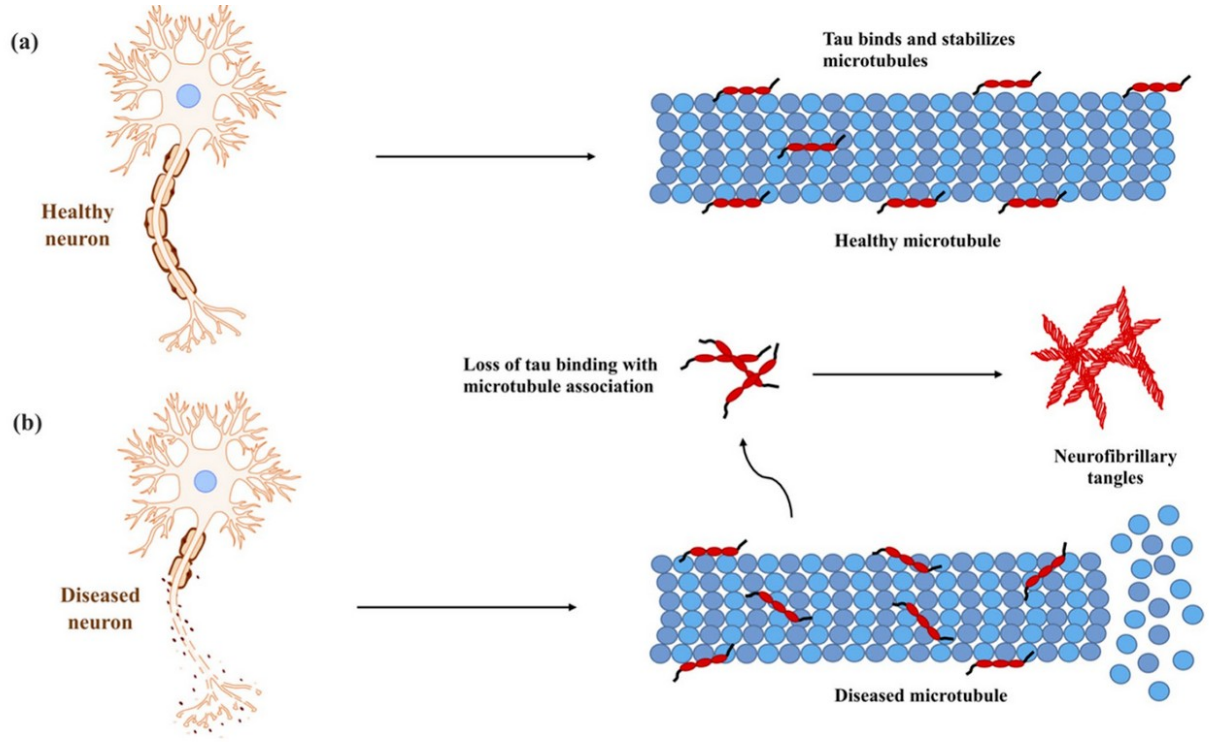

Figure 6. Tau function in healthy neurons and tauopathy disease states. (A) Tau binds to and stabilizes microtubules in healthy neurons. (B) In tauopathy disease states, tau losses its ability to bind to microtubules and forms NFTs. Figure adapted from Kaur et al., 2022.

Different tau isoforms can also change how tau is able to interact with microtubules. Tau has six different isoforms found in the CNS. Inclusion or exclusion of exons 2, 3, and 10 when

splicing the microtubule-associated protein tau (MAPT) gene can result in three different N-terminal inserts (N0, N1, N2) and two different C-terminal microtubule-binding repeat domains (3R, 4R) (Fig. 7) (Vourkou et al., 2022). 4R tau isoforms are found to bind more effectively to microtubules than the 3R tau isoforms due to the extra microtubule binding repeat insertion (Panda et al., 2003). Both 3R and 4R tau isoforms are found at equivalent levels within the CNS (Vourkou et al., 2022).

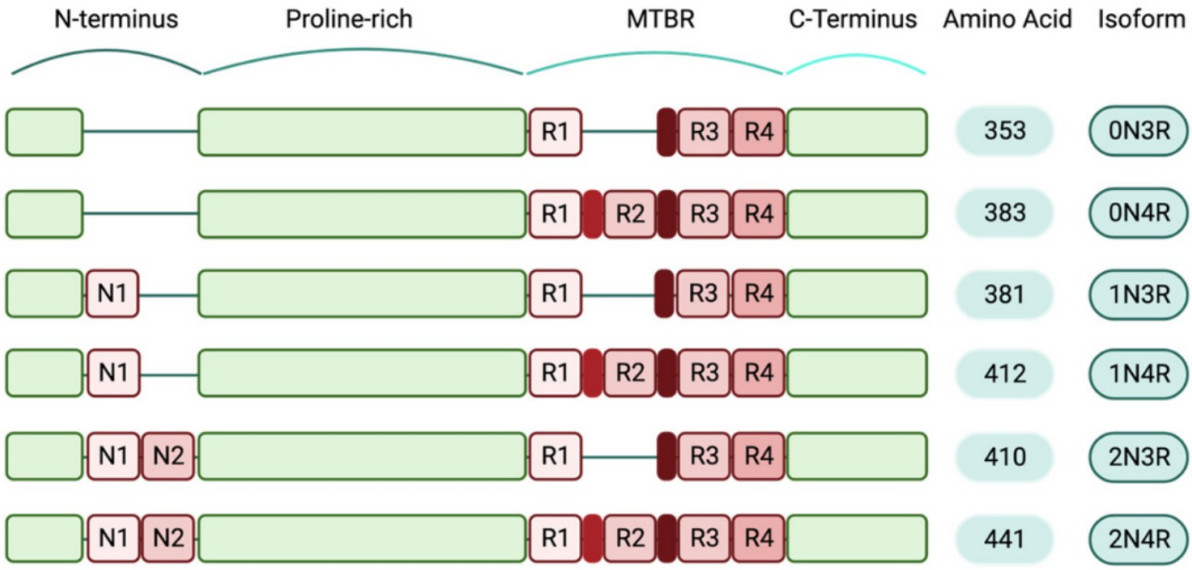

Figure 7. Six different tau protein isoforms form from alternative splicing of the MAPT gene. Tau isoforms can be alternatively spliced by inserting two different N-terminus inserts (N1 or N2) or lack an N-terminus insert (N0). Tau isoforms can also contain different numbers of microtubule binding repeats (3R or 4R). This results in the six tau isoforms identified by both the number of N-terminus inserts and the number of microtubule binding repeats (0N3R, 0N4R, 1N3R, 1N4R, 2N3R, or 2N4R). Tau isoforms range from 353 to 441 amino acids in length. Figure adapted from Tabeshmehr & Eftekharpour, 2023.

2.2 Tauopathies in Humans

Tauopathies are neurodegenerative diseases characterized by the presence of sarkosyl insoluble aggregates of hyper-phosphorylated tau in neurons and glia. Tauopathies include but are not limited to: Alzheimer's disease (AD), frontotemporal dementia (FTD), Pick's Disease (PiD) corticobasal degeneration (CBD), and progressive supranuclear palsy (PSP). Tau aggregates within these diseases can affect both neurons and glia. Tau aggregates within neurons are referred to as neurofibrillary tangles (NFTs), and tau tangles within glia are referred to as glial fibrillary tangles. Tau aggregates within cells are believed to be toxic to the cell they exist in, as hyperphosphorylated tau can promote microtubule disruption (Alonso et al., 2018), synaptic loss, (Bloom, 2014), DNA damage (Frost et al., 2014), mitochondrial dysfunction

(Schulz et al., 2012), and even cell death (Arendt, 2012). In addition to the toxicity related to cellular atrophy, the amount of neurofibrillary tangles found, and the degree of cognitive impairment of patients with Alzheimer's, is strongly correlated (Braskie et al., 2011).

Each different tauopathy has unique disease features related to the cells the tauopathy effects and the localization of tau-positive inclusions. While the neuron has been the central focus of research within understanding neurodegeneration, glial cells are also affected by tau toxicity. Some tauopathies have disease pathology that results in different morphological and functional changes to astrocytes and glia in addition to neuronal cell death. While less researched, glial fibrillary tangles in astrocytes and oligodendrocytes are thought to be similarly toxic to the glial cells they inhabit compared to NFTs. Each tauopathy has a different ratio of tau tangle accumulation between neuron and glia. Glial fibrillary tangles have been found most prominently in tauopathies such as CBD (Feany and Dickson, 1995), and PSP (Kovacs et al., 2020).

Beyond what has been observed with tauopathy-specific glial tau pathology, there is also an astrocytic specific tau pathology that is more general across tauopathies. These astrocytic tau accumulations have been encompassed under the umbrella term of ARTAG, or aging-related tau astrogliopathy (Kovacs et al., 2016). ARTAG includes tau-positive astrocyte morphologies that are prominent in the tauopathies CBD, PSP, and PiD as astrocytic plaques, tufted astrocytes, and ramified astrocytes, respectively (Fig. 8). In addition, more general tau-positive inclusions like globular astroglial inclusions, thorn-shaped astrocytes, and granular or fuzzy tau immunoreactivity are also found in processes of astrocytes, and are classified under the ARTAG umbrella.

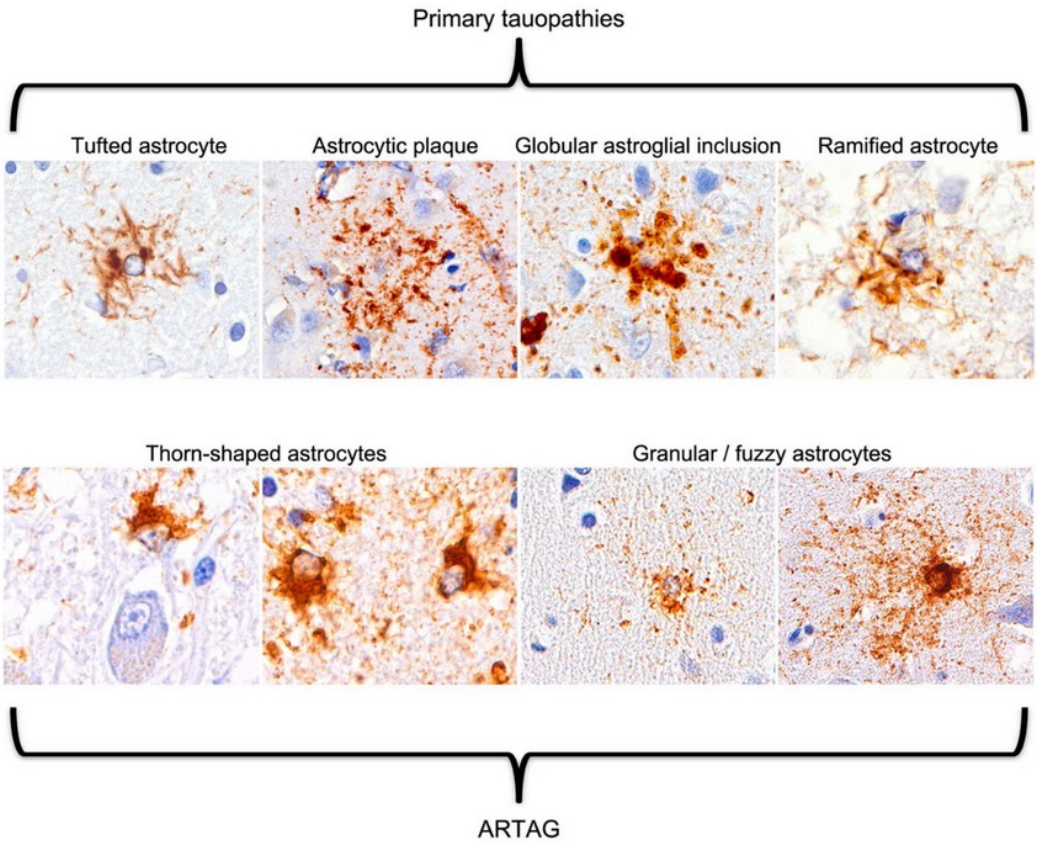

Figure 8. ARTAG encompasses tau-immunoreactive cytoskeletal morphological changes to astrocytes across different tauopathies. Tufted astrocytes are exclusive to PSP pathology. Astrocytic plaques are exclusive to CBD pathology. Globular astroglial inclusions are found in globular glial tauopathy (GGT). Ramified astrocytes are exclusive to Pick's Disease pathology. Thorn-shaped astrocytes and granular/fuzzy astrocytes are not specific to any one tauopathy pathology and can be found across different tauopathies. While the specific morphologies can be unique to different diseases, aspects of ARTAG are present across primary tauopathies. Figure adapted from Kovacs et al., 2016

Tau pathology can also differ in the tau isoform that is accumulating in tau tangles (3R or 4R). Tau tangles of the 3R and 4R tau isoforms are found to be equally distributed in Alzheimer's, but tau tangles of the 4R isoform are the only tau isoform in tangles in PSP (Kovacs et al., 2020). Different tauopathies can contain tau aggregates of the 3R isoform, 4R isoform, or a combination of both (Fig. 9). Tau aggregates of the 4R isoform are considered to be more toxic than the 3R isoforms. Experiments done in fruit flies showed overexpression of the 3R isoform results in locomotor impairment and axonal transport deficits, whereas overexpression of the 4R isoform results in impairments to learning and memory and amplified neurodegeneration (Sealey et al., 2017; Vourkou et al., 2022).

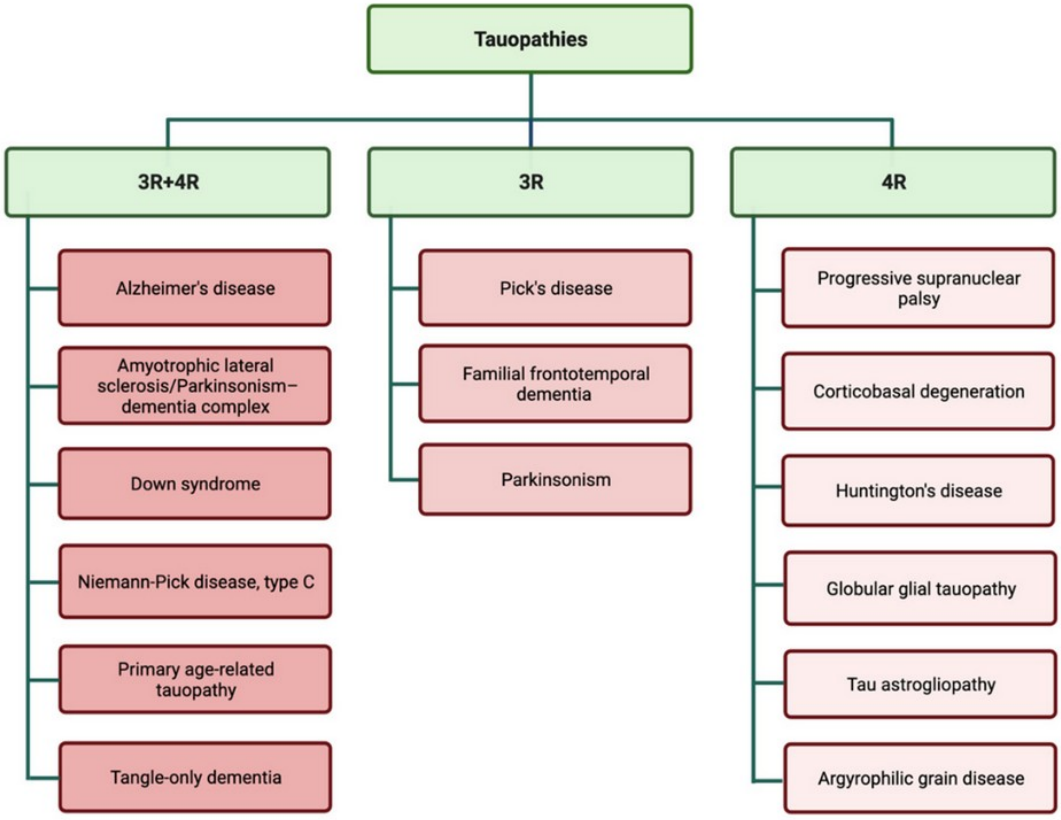

Figure 9. Tauopathies can differ based on the isoform of aggregated tau. Tauopathies can be classified based on what tau isoform is present in tau tangles. Alzheimer's has an equal amount of 3R and 4R tau tangles. 3R tauopathies include FTD and PiD, 4R tauopathies include PSP and CBD. Figure adapted from Tabeshmehr & Eftekharpour, 2023.

Mitochondrial dysfunction is associated with neurodegenerative disorders such as Alzheimer's Disease (Klemmensen et al., 2024; Wang et al., 2020), CBD (Valentino et al., 2020), PSP (Albers et al., 2001; Valentino et al., 2020), and FTD (Anoar et al., 2021). Disorders that impair mitochondrial function inherently impair cellular respiration. Cellular respiration requires the mitochondria organelle to generate ATP (Voet & Voet, 2006). Mitochondria move across cytoskeletal tracts to different locations of the cell to produce ATP in areas where ATP is needed in abundance. An example of this is at the synapse, where an abundance of ATP is needed to release synaptic vesicles (Kramer & Bressan, 2018; Rossi & Pekkurnaz, 2019).

In addition to a lack of ATP, mitochondria dysfunction results in an increase in ROS within the cell. ROS is a toxic byproduct of aerobic cellular respiration produced within mitochondria (Zhang et al., 2022). Under healthy conditions, mitochondria convert its ROS byproduct to H_2O through superoxide dismutase (SOD), peroxiredoxin (PRX), and glutathione

peroxidase (GPX) (Zhang et al., 2022). Increased ROS is observed in normal aging and exacerbated in tauopathy disease states (Ionescu-Tucker & Cotman, 2021), this suggests that impaired mitochondrial function in tauopathies limits its ability to neutralize ROS.

One side effect of increased ROS within the cell is DNA damage. DNA damage caused by ROS can take three different forms: single strand base damage, single stranded nick, or double stranded breaks (DSBs). Moreover, single stranded nicks can also become DSBs during DNA replication (Karanjawala & Lieber, 2004). DSBs can be repaired by either homologous recombination functions in dividing cells or non-homologous end joining (NHEJ). However, continued exposure to ROS will result in persistent DSBs, that if left unrepaired will lead to cellular senescence (Chen et al., 2007).

Tau aggregates are indirectly responsible for DNA damage due to impaired mitochondria function. Furthermore, there is a strong association between the presence of NFTs and cellular senescence (Musi et al., 2018). Other studies found that oxidative stress-induced DNA damage due to tau pathology results in heterochromatin relaxation (Frost et al., 2014). This is consistent with cellular senescence observed in tauopathies, as chromatin undergoes global relaxation when DNA damage occurs to allow for amplification of the DNA damage repair response (DDR) (Lemaître & Soutoglou, 2014).

While oxidative stress-induced DNA damage and cellular senescence are a part of these diseases, it is unclear the exact mechanism by which these tau tangles may inhibit mitochondria function. Animal models can be useful in accelerating knowledge about pathological features of neurodegeneration such as mass neuronal death, cell cycle arrest, and respiratory deficits, that can potentially be applied to produce treatments for these disorders.

2.3 Tauopathy Models in Fruit Flies

Fruit fly models of tauopathies are modeling primary tauopathies. Primary tauopathies are neurodegenerative disorders in which the tau abnormalities are the primary pathology to a disease (Khurana, 2008). CBD, PSP, PiD, and FTD are all examples of primary tauopathies. Alzhiemer's disease is considered a secondary tauopathy due to amyloid deposits that are found in conjunction with tau tangles (Selkoe, 2001). It is also important to note that glial cells develop

tau abnormalities in primary tauopathies, compared to secondary tauopathies like Alzhiemer's, in which glia primarily remain unaffected by abnormal tau accumulation.

Modeling primary tauopathies in flies have furthered the understanding of how glia are implicated within these diseases. An experiment done with fruit flies over-expressing tau in all glial cells used deoxynucleotidyl transferase dUTP nick end labeling (TUNEL) assays to mark the DNA of glial cells that have undergone apoptosis. In the same experiment, neuronal cell death was also seen using the cholinergic neuronal cytoplasmic marker, choline acetyltransferase (ChAT). Cholinergic neurons were targeted due to the hypothesis that cholinergic neuron loss and/or dysfunction is associated with Alzheimer's disease in humans (Bartus et al., 1982). The overlap found between TUNEL-positive cells and ChAT-positive cells shows that cholinergic neuronal death is present in flies overexpressing tau only in glial cells (Colodner & Feany, 2010). Moreover, flies with glial cells over-expressing tau had a significantly reduced lifespan compared to control flies, further highlighting this toxicity.

Fruit fly models of tauopathies have also led to the discovery of primary tauopathy association with abnormal cell cycle activity. A previous thesis done in Colodner Lab at Mount Holyoke College by Rachel Sunwoo Kang showed that astrocyte specific tau-overexpression in fruit flies results in an increase in astrocytes in day 3 female flies, but not in day 3 male flies (Kang, 2023). Immunostaining these flies for cell proliferation marker, Proliferating cell nuclear antigen (PCNA), showed female flies overexpressing tau in astrocytes had higher levels of PCNA markers compared to LacZ controls (Kang, 2023). Other studies have found that cell cycle markers are abnormally expressed in brains of flies overexpressing tau in all neurons, and that this repeated ectopic cell cycle activation may be contributing to neuronal apoptosis (Khurana, 2008; Khurana et al., 2006). These findings highlight the importance of investigating cell cycle activity in tau pathology.

Chapter 3: Aim of Study

The overall aim of this study is to determine whether astrocytic tau expression impairs respiration in the fly brain to better define how tauopathies may impact cellular respiration. The methods used in this project will examine respiration rate of flies with tau-overexpression in astrocytes compared to the respiration rate of control flies across age and sex. The hypothesis posited for this project is that respiration rate will decrease with age in flies with tau-overexpressing astrocytes compared to the baseline respiration rate. This is posited due to the damage tau aggregates cause to the cell may compromise possible cellular functions, such as the astrocytic modulation of respiration. Additional experiments will explore the relationship between cell cycle arrest and related cellular senescence markers, in control flies and flies over-expressing tau in astrocytes. These experiments will pave the way for future research into the possible role that cellular senescence has on respiration.

MATERIALS AND METHODS

1. *Drosophila melanogaster* model animal

1.1 UAS-GAL4 System

The UAS-GAL4 system is a gene manipulation method most commonly used in fruit flies to genetically target and alter protein expression in specific cells (Fig. 10) (Brand & Perrimon, 1993). GAL4 is a transcription factor observed in baker's yeast (*Saccharomyces cerevisiae*) that contains a DNA-binding domain and an activation domain. The DNA-binding domain can attach itself to DNA that encodes for a specific protein, most commonly cell-specific proteins. This is referred to as a "driver" or promoter gene. The activation domain of GAL4 binds to an upstream activation sequence (UAS), which can then activate gene transcription of reporter gene X downstream from UAS. If the DNA of a fly contains both Y-GAL4 and UAS-X, then GAL4 will bind to the UAS to produce protein X expression under the control of the Y promoter. It is important to note that DNA containing Y-GAL4 or UAS-X alone will not genetically alter protein expression in any promoter, as GAL4 and UAS must be paired together in order to work.

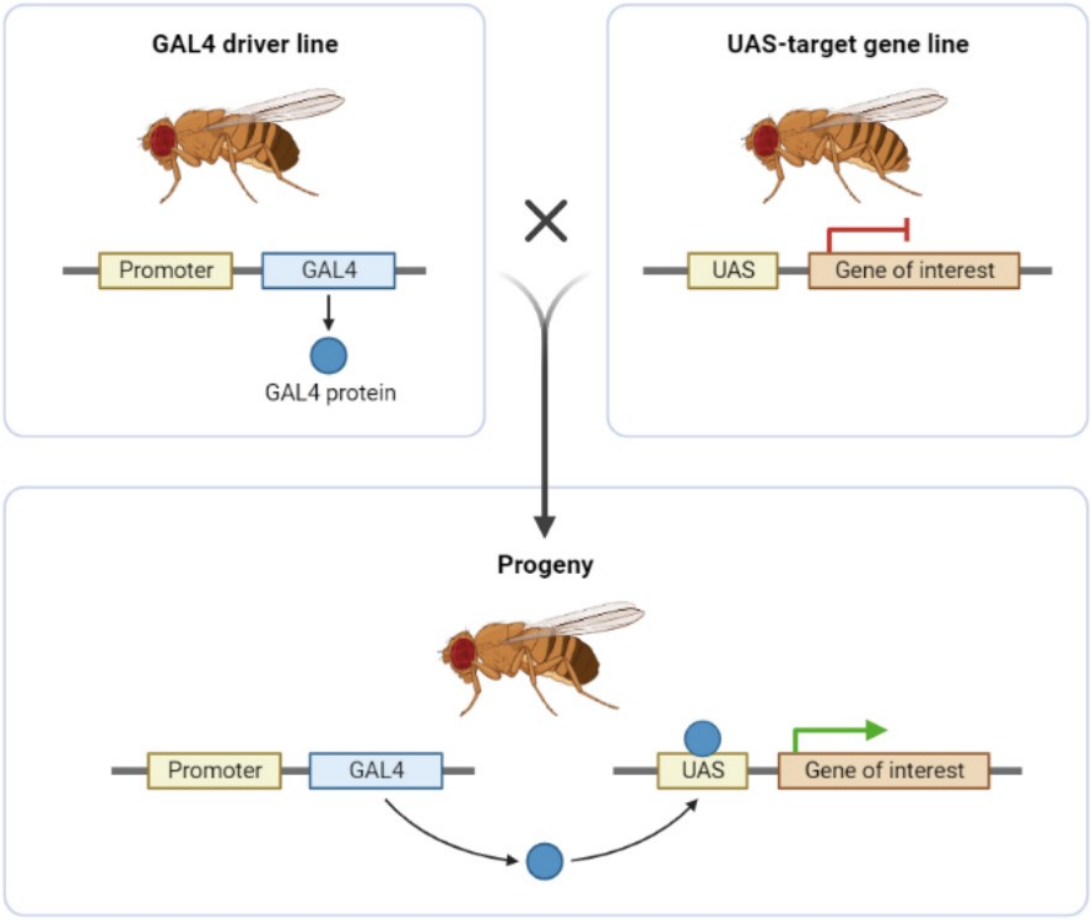

Figure 10. Tissue-specific gene expression in *Drosophila melanogaster* can be accomplished using the GAL4/UAS system. A tissue-specific promoter is attached to the GAL4 transcription factor. This GAL4 protein binds to and activates UAS, which when attached to the gene of interest, will produce progeny expressing a target gene in the specific tissue. Figure from Sally Kim, artist depiction.

1.2 *Drosophila melanogaster* husbandry and stocks

All fly stocks were housed in 25 degree celsius incubators, excluding virgins collected from stocks that were kept in 17 degree celsius incubators until a genetic cross was set up. Flies were kept in plastic vials with Nutri Fly fly food at the bottom, along with a few specks of yeast to promote breeding. Some experiments were conducted with molasses-based food as the primary diet, but at least three days prior to an experiment flies were placed in vials containing cornmeal-based Nutri Fly food. The Nutri Fly food contains added tegosept and propionic acid to prevent fungal growth in the fly vials.

1.3 Genetic Crosses

To set up genetic crosses between flies of different genotypes, 4-6 virgin female flies of X genetic makeup and 4-6 male flies of Y genetic makeup are placed together in a vial with bits of yeast to promote breeding. Every 7 days, the parents are flipped to a new vial to prevent cross-breeding between parent and progeny. Progeny emerges approximately 10 days after the cross is initially set up. Progeny are then collected from the vial for 8 days to ensure the genetic makeup results from the parents, and not from other progeny.

The cell-specific promoter used in the GAL4 construct to target astrocytes was the astrocyte leucine-rich repeat molecule (alrm) gene. The crosses used for these experiments are UAS-tau X alrm-GAL4, UAS-tau X W-, alrm-GAL4 X W-. UAS-tau X alrm-GAL4 is the experimental cross that will produce progeny overexpressing hTau in astrocytes. Flies that result from the UAS-tau X alrm-GAL4 cross may be referred to as tau flies. UAS-tau X W- and alrm-GAL4 X W- are control crosses to ensure any respiratory effects observed in experiments are not due to the insertion of GAL4 into the fly's chromosomes.

2. Respirometry

2.1 3D Printing and Stand Construction

3D printing was done with the assistance of staff at Fimbel Lab located at Mount Holyoke College. Respirometry racks and a camera stand were adapted and edited in Fusion 360 from an original design created from Botero *et al.,* 2021 . The respirometry rack was printed in glass fiber material on an XRize 3D printer. Later experiments included a revised respirometry rack made from PVC plastic and printed on a Raise 3D Pro Plus 3d printer. The camera stand was printed in PLA plastic on an Ultimaker s5 3D printer, then glued to a wooden board to ensure it is always 22 cm away from the respirometry tank.

2.2 Volumetric Respirometer Construction

The construction of the individual volumetric respirometers was adapted from the protocol described in Yatsenko *et al.,* 2014. Each respirometer consists of a p1000 pipette tip and a 50 µl capillary tube. The p1000 pipette tip end was severed with a razor blade to ensure the capillary tube fit snugly. The respirometer was then made airtight by applying glue to the end of the capillary tube and placing it back in the hole of the pipette tip, twisting the capillary tube slightly out while the glue hardened. Once glued together, the pipette tip of the respirometer was then placed between two magnets above a lab bench to ensure even, straight drying. Once dry, a small piece of foam is placed at the bottom of each respirometer tip followed by a few pieces of soda lime followed by an additional piece of foam to separate the flies from directly touching the soda lime (Fig. 11).

2.3 CO2 Measurement using Volumetric Respirometry

Flies to be tested were assured to have no CO_2 anesthetic exposure at least 24 hours before an experiment. To load flies into each respirometer, flies were iced and then quickly sorted and separated by genotype and sex. Each individual respirometer contained exactly four flies of the same sex and genotype. Up to sixteen of these respirometers fit in the respirometry rack. Respirometers were then capped off with a plasticine putty seal on the micropipette tip. The respirometry rack was then placed inside a large, rectangular TLC chamber filled with 800 mL of red food dye solution (Fig. 11). This apparatus was then moved into a temperature control

chamber set to 25 degrees celsius, where the lid for the chamber was sealed using vacuum grease, then it was placed in its appropriate spot on the wooden board 22 cm away from the camera.

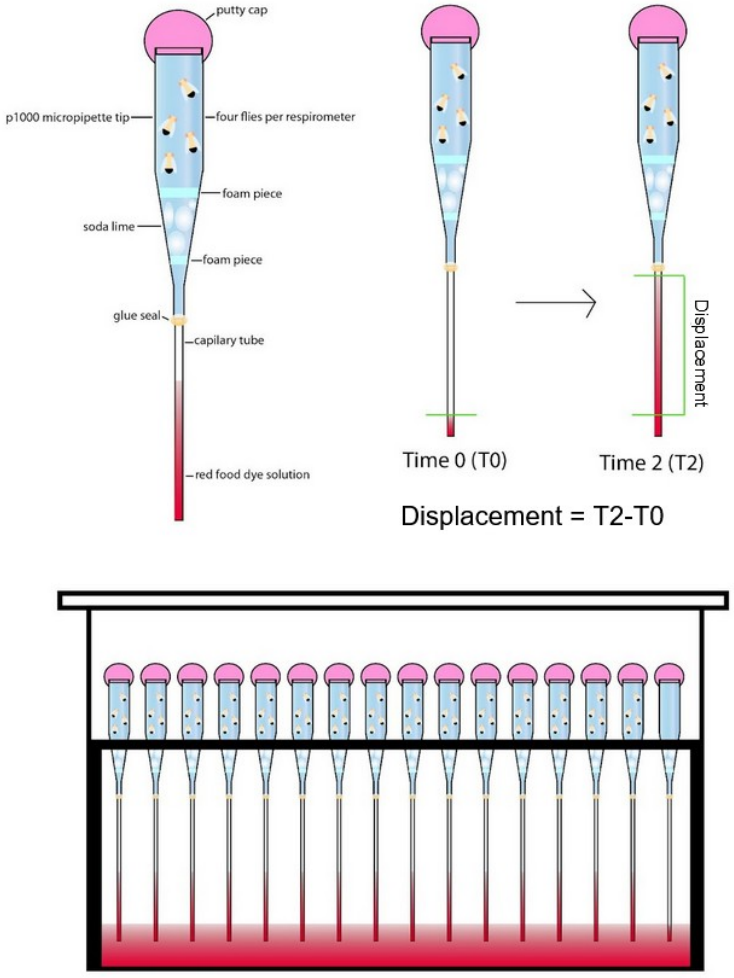

Figure 11. The respirometry apparatus: visualizing the experimental setup.
Each respirometer is made from a p1000 micropipette tip and a 50 µl capillary tube glued together. The p1000 tip contains bits of soda lime in between two pieces of foam. The displacement of the liquid is taken from the liquid level at T0 subtracted from the liquid level at T2. This displacement is an indirect measure of the oxygen taken in by the flies over a two hour period of time.

2.4 Time Lapse Image Capture and Data Analysis

The camera captured images every fifteen minutes using the time lapse image capture tool in Phenocapture. All experiments were started between 9:00 am and 1:00 pm, with the first three hours existing as the acclimation period for the flies, and the last two hours as the experiment run time. The acclimation period is crucial as the liquid in each capillary must reach

above the water level to be considered a start point for analysis. Data was analyzed using Image J by measuring the meniscus of each capillary tube at the end of the experiment run time and calculated the difference from the meniscus of each capillary tube at the start of the experiment run time.

3. Immunofluorescence

3.1 Brain Dissection

Flies were aged to days 3, 10, or 20, separated by sex and genotype and anesthetized with ice the day of the dissection. Each fly was dipped in 70% ethanol for three seconds followed by two quick dips in phosphate-buffered saline (PBS), then transferred to a non-lobind tube with 500 µL of perfluoroalkoxy alkane (PFA) for 15 minutes. PFA was then pipetted out of the non-lobind tube and replaced with PBS. PBS washing occurred twice more before being placed on ice. Flies were then dissected under a simple light microscope using forceps. The body was first removed from the head, then the proboscis was removed leaving a hollow space between the cuticle and the brain. The cuticle was then carefully removed to expose the brain. The external trachea was left intact. Each brain was transferred into a Terasaki well plate with 10 µL of PFA. The first brain dissected spent the most time in the PFA solution, up to 50 minutes.

3.2 Immunostaining

After dissection, PFA was pipetted out of each well and rinsed with PBS twice. The brains were then washed twice with PBS for 20 minutes while nutating at room temperature. After both washes, PBS was removed from all wells and replaced with 10 µL of PBS 0.5% Triton X-100 (PBT) for 20 minutes while nutating at room temperature. PBT was then removed and then replaced with 10 µL of a PBT + 5% NGS blocking solution (190µL PBT + 10µL Normal Goat Serum) per well, and nutated for 90 minutes at room temperature. After 90 minutes, blocking solution was removed. Primary antibody MS α his2av was diluted in blocking solution at a 1:100 ratio (1µL MS α his2av in 100µL of PBT+5%NGS), then added to each well in the Terasaki plate. The primary antibody nutated with the brains in the well plate for 2 hours at room temperature, then overnight at 4 degrees celsius. After overnight nutation, the primary antibody was removed and replaced with PBT for 4 washes of 15 minutes while nutating. After the washes were completed, PBT was removed and the secondary antibody Alexa 488 Goat α Mouse in a 1:200 dilution (1 µL antibody in 200µL of PBT+5%NGS) was added to each well. The secondary antibody nutated with the brains in the well plate for 2 hours at room temperature, then overnight at 4 degrees celsius. After overnight nutation, the secondary antibody was removed and replaced with PBT for 4 washes of 15 minutes while nutating. Each well was rinsed

with PBS. 40% glycerol was added to each well and nutated for 10 minutes, then removed. 60% glycerol was added to each well and nutated for 10 minutes, then removed. 80% glycerol was added to each well and nutated for 10 minutes, then removed.

3.3 Slide Mounting

10µL of Vectashield with DAPI was added to each well in the Terasaki plate. Slides were constructed with a bridge consisting of two halves of a broken coverslip glued to a slide. 50µL of Vectashield with DAPI was pipetted onto the middle of each slide labeled with corresponding sex and genotype. Brains were pipetted from well plate onto slides, and a coverslip was glued on over the bridge pieces.

3.4 Confocal Imaging

Confocal imaging was done of slides containing fly brains using a laser-scanning Nikon Ti2 confocal microscope at the 20x objective with a 2µm interval between focal planes. The top and bottom of the z-stack was set by scrolling through the brain volume until the first focal plane with no fluorescent signal visible was found. Once the z-stack was set, samples were imaged following the order of experiment: Large Image, Lambda, Z-series. This means that the microscope captures the image size first, then the laser line, then each section within the z-stack. Samples were imaged utilizing two sequential laser lines; DAPI (blue) and GFP (green). The DAPI laser line was set to laser equals 20, gain equals 30. The GFP laser line was set to laser equals 7, gain equals 10. The DAPI laser line visualized the cell nuclei, which fluoressed blue from the addition of Vectashield with DAPI during the mounting process. The GFP laser line visualized the secondary antibody, Goat anti-mouse Alexa 488, attached to the primary antibody MS α his2av, used to visualize double-stranded breaks within DNA. Images collected from this process were saved as an nd2 file and imported to ImageJ.

3.5 ImageJ Pseudo-coloring

Nd2 files imported to ImageJ were uploaded as composite images in an attempt to keep image data intact from the original file. Each file was split into two fluorescent channels using the split channels command. Lookup tables were used to add pseudo color to each channel, either blue for DAPI or green for GFP. Z-projections were then made for each channel using the

z-project command and selecting the max intensity option. Z-projections were rotated accordingly to have the brain's dorsal side be upwards and the brain's ventral side be downwards. Scale bars were added to each image. Merged z-projections were formed by merging both channels using the merge channel function. Pseudo-colored images were then exported as a JPEG.

4. Statistical Analysis

Data was collected from the experimental apparatus described in the Materials and Methods section. This study's population will be *Drosophila melanogaster*, commonly known as the fruit fly. The genetic backgrounds of flies used were of the *w*- background. Any genetic crosses (control or experimental) were done using flies from a *w*- genetic background. This study measures respiration rate, and aims to look at how respiration rates may change with certain variables altered. The variables that were examined are sex, age, and experimental genetic crosses (overexpressing hTau in astrocytes).

A power analysis calculated through the pwr package for R determined the sample size needed to assess how the variables examined impact respiration rate. Using Cohen's (1988) criteria with a significance criterion of $\alpha = .05$, power = .50, and Cohen's $F = 0.8010605$, the minimum sample size needed with this effect size is $n = 4$ to assess how the sex variable impacts respiration rate. To determine the sample size needed to assess how the age variable impacts respiration rate using $\alpha = .05$, power = .50, and Cohen's $F = 0.04815568$, the minimum sample size needed with this effect size is $n = 713$. This sample size needed is impossible to obtain within the time constraints of this project, suggesting that the age variable has little effect on respiration rate. Lastly, to determine the sample size needed to assess how the genotype variable impacts respiration rate using $\alpha = .05$, power = .50, and Cohen's $F = 0.08089342$, the minimum sample size needed with this effect size is $n = 179$. This sample size needed is difficult to obtain within the time constraints of this project, suggesting that the genotype variable also has little effect on respiration rate. Given the high sample size needed for both age and genotype variables, the sex sample size was used as the minimum amount for each group of the same age, sex, and genotype. Previous research looking at respiration rate in fruit flies using the same volumetric respirometric method had a sample size between 5 and 14 per genotype (Botero et al., 2021).

To test whether or not sex has an effect on respiration rate, a one-way ANOVA was used to compare respiration rate of males and females. To test the hypothesis of increased respiration rates for flies overexpressing hTau in astrocytes, the experimental genetic crosses that result in overexpressed hTau in astrocytes was compared to the combined average respiration rate of both genetic control crosses in each age category for each sex using a two-way ANOVA. To test the possible role age has in respiration rate across genotypes, a one-way ANOVA was used. All

statistical analysis was done in R studio with various packages including pwr, dplyr, ggplot, rstatix, EnvStats, and ggpubr (Appendix).

RESULTS

1. Sex differences observed in respiration rate

To determine if there are sex differences in respiration rate, flies were sorted by sex for volumetric respirometry to determine respiration rate. Combining all genotypes and ages, sex does have a significant effect on respiration rate (Fig. 12) and all further analysis will treat the respiration patterns of male and female flies as sex-specific patterns.

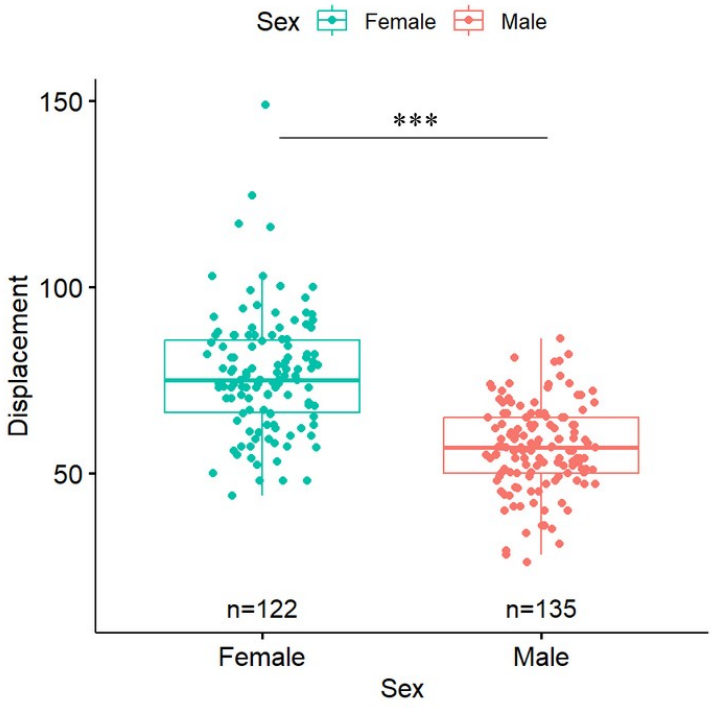

Figure 12. Females have a higher respiration rate than males. The displacement is an indirect measure of respiration determined by volumetric respirometry. Across sexes, females (n = 122) had a significantly higher respiration rate than males (n = 135). Statistical analysis was performed using a one-way ANOVA [$F(1, 255) = 132.1$, $p < 2.2e\text{-}16$]. Signif. codes *p < 0.05, **p < 0.01, ***p < 0.001

2. Astrocytic tau overexpression increases respiration rate in day 3 female flies

To test the hypothesis that astrocytic tau overexpression alters respiration rate for each sex group, the respiration rate of the female control group was compared to the female tau group at each age point using a two-way ANOVA. There was no significant difference found in respiration rate between the tau and control groups at day 10 and day 20, but there was a significant difference in respiration rate between tau and control groups at day 3 (Fig. 13).

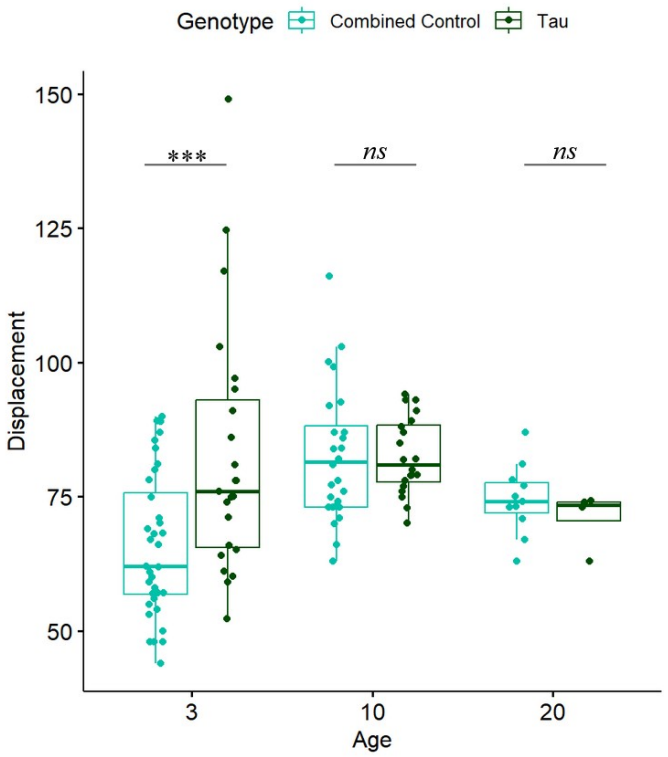

Figure 13. Astrocytic tau overexpression increases respiration in day 3 female flies. The displacement is an indirect measure of respiration determined by volumetric respirometry. Statistical analysis was performed using a two-way ANOVA to assess the genotype and age effect on respiration [$F(2, 116) = 5.609$ $p = 0.00473$]. Post hoc comparisons using a Tukey HSD test found that day 3 female tau flies ($n = 23$) have a significantly higher respiration rate compared to day 3 female control flies ($n = 36$) ($p = 0.0003543$). No difference was found in respiration rate between day 10 female tau flies ($n = 20$) and day 10 female control flies ($n = 28$) ($p = 0.9999974$) or day 20 female tau flies ($n = 4$) and day 20 female control flies ($n = 11$) ($p = 0.9984972$).

3. Astrocytic tau overexpression has no effect on respiration rate in males

To test the hypothesis that astrocytic tau overexpression alters respiration rate of males, the respiration rate of the male control group was compared to the male tau group at each age point using a two-way ANOVA. There was no significant difference found in respiration rate between the tau and control groups at any age (Fig. 14).

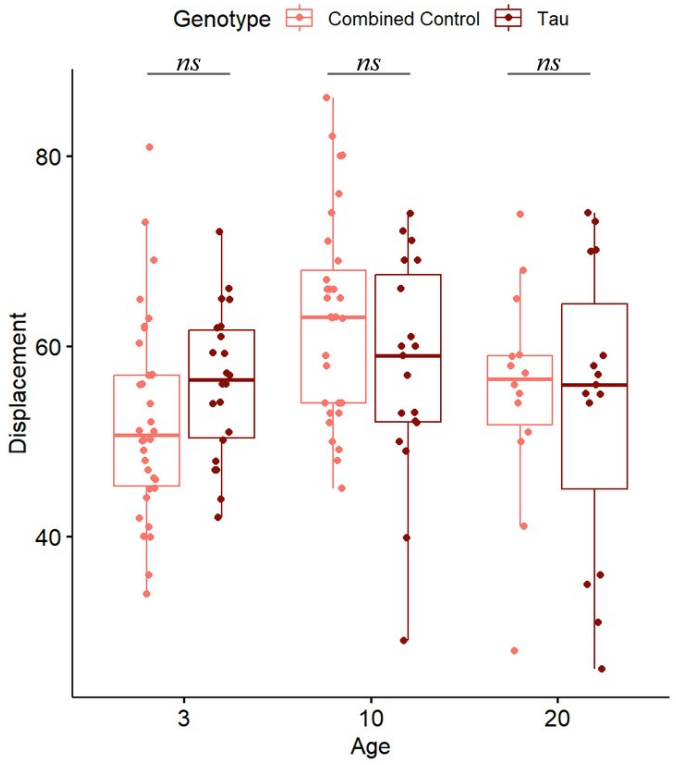

Figure 14. Astrocytic tau overexpression has no effect on respiration in males. The displacement is an indirect measure of respiration determined by volumetric respirometry. Statistical analysis was performed using a two-way ANOVA to assess the genotype and age effect on respiration [$F(2, 129) = 2.205$ $p = 0.11443$]. Post hoc comparisons using a Tukey HSD test found no significant difference in respiration rate of day 3 male tau flies ($n = 22$) and day 3 male control flies ($n = 34$) ($p = 0.8112386$), no significant difference in respiration rate of day 10 male tau flies ($n = 19$) and day 10 male control flies ($n = 31$) ($p = 0.5374536$), and no significant difference in respiration rate of day 20 male tau flies ($n = 15$) compared to day 20 male control flies ($n = 14$) ($p = 0.9993219$).

4. Female control flies show increased respiration from day 3 to day 10

To further assess respiration rate changes across age, one-way ANOVAs were used to compare how respiration rate changes across age groups in each genotype. There was a significant difference in respiration rate between day 3 and day 10 female control flies. There was no significant difference in respiration rate between day 10 and day 20 or day 3 and day 20 (Fig. 15).

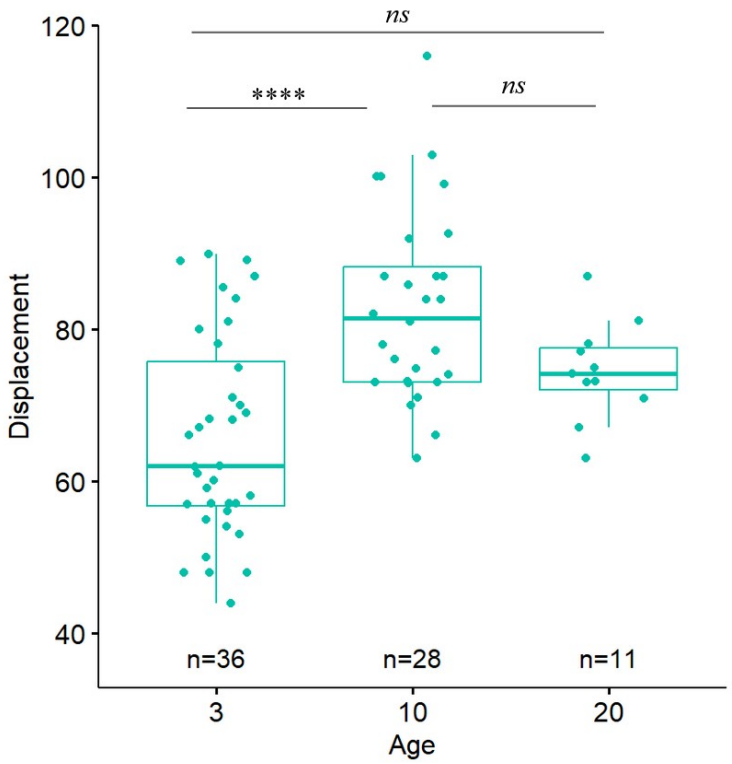

Figure 15. Female control flies show increase in respiration from day 3 to day 10. The displacement is an indirect measure of respiration determined by volumetric respirometry. Statistical analysis was performed using a one-way ANOVA [F(2, 72) = 15.6, p = 2.35e-06]. Post hoc comparisons using a Tukey HSD test found that day 10 female control flies (n = 28) have a significantly higher respiration rate compared to day 3 female control flies (n = 36) (p = 0.0000012). There is no significant difference in respiration rate of day 10 female control flies compared to day 20 female control flies (n = 11) (p = 0.1361597). There is also no significant difference in respiration rate of day 3 female control flies compared to day 20 female control flies (p = 0.1012190).

5. Female tau flies do not have respiration rate differences across aging

To further assess respiration rate changes across age, one-way ANOVAs were used to compare how respiration rate changes across age groups in each genotype. For female tau flies, there was no significant difference in respiration rate between day 3 and day 10, day 10 and day 20, or day 3 and day 20 (Fig. 16).

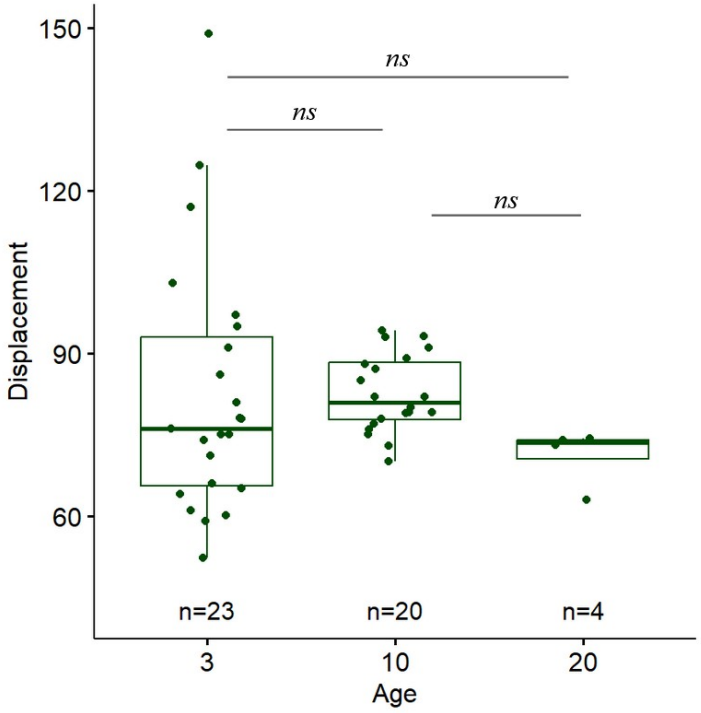

Figure 16. Female flies overexpressing astrocytic tau do not have respiration rate differences across ages. The displacement is an indirect measure of respiration determined by volumetric respirometry. Statistical analysis was performed using a one-way ANOVA [F(2, 44) = 0.808, p = 0.452]. Post hoc comparisons using a Tukey HSD test found that there is no significant difference in respiration rate of day 3 female tau flies (n = 23) compared to day 10 female tau flies (n = 20) (p = 0.9999852), no significant difference in respiration rate of day 10 female tau flies compared to day 20 female tau flies (n = 4) (p = 0.4526328), and no significant difference in respiration rate of day 3 female tau flies compared to day 20 female tau flies (p = 0.4432112)

6. Male control flies show increased respiration from day 3 to day 10

To further assess respiration rate changes across age, one-way ANOVAs were used to compare how respiration rate changes across age groups in each genotype. There was a significant difference in respiration rate between day 3 and day 10 male control flies. There was no significant difference in respiration rate between day 10 and day 20 or day 3 and day 20 male control flies (Fig. 17).

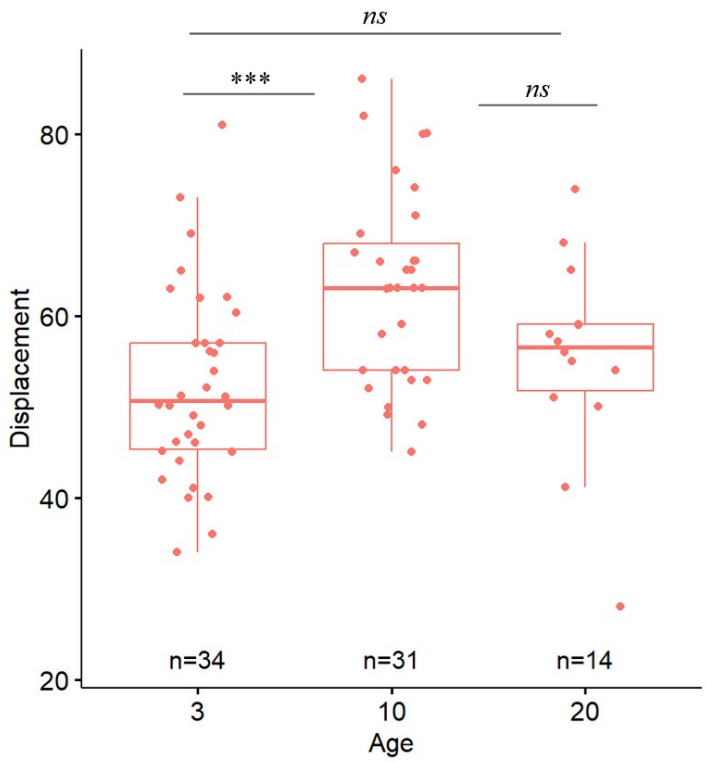

Figure 17. Male control flies show increase in respiration from day 3 to day 10. The displacement is an indirect measure of respiration determined by volumetric respirometry. Statistical analysis was performed using a one-way ANOVA [F(2, 76) = 8.494, p = 0.000468]. Post hoc comparisons using a Tukey HSD test found that there is a significant difference in respiration rate of day 3 male control flies (n = 34) compared to day 10 male control flies (n = 31) (p = 0.0003377), but no significant difference in respiration rate of day 10 male control flies compared to day 20 male control flies (n = 14) (p = 0.0678986), and no significant difference in respiration rate of day 3 male control flies compared to day 20 male control flies (p = 0.6492178).

7. Male tau flies do not have respiration rate differences across aging

To further assess respiration rate changes across age, one-way ANOVAs were used to compare how respiration rate changes across age groups in each genotype. For male tau flies, there was no significant difference in respiration rate between day 3 and day 10, day 10 and day 20, or day 3 and day 20 (Fig. 18).

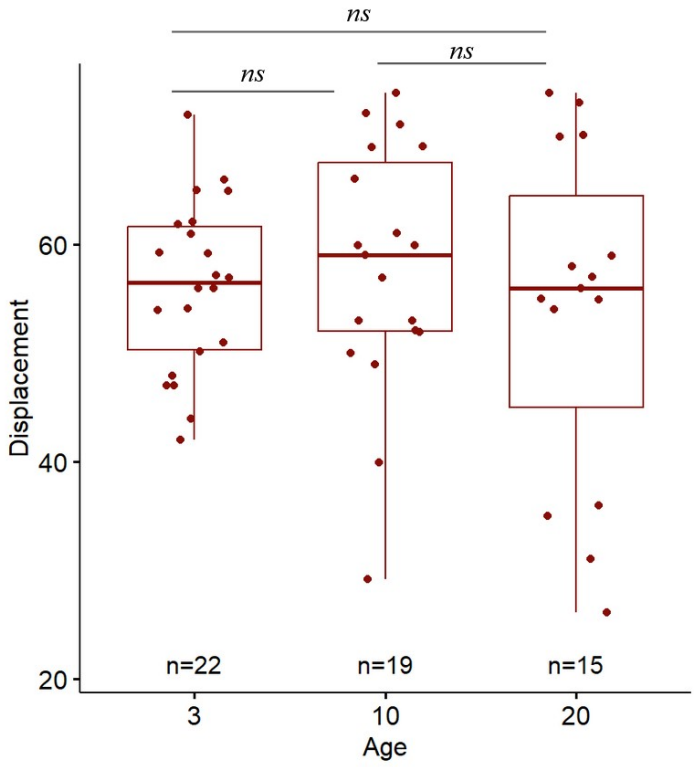

Figure 18. Male flies overexpressing astrocytic tau do not have respiration rate differences across ages. The displacement is an indirect measure of respiration determined by volumetric respirometry. Statistical analysis was performed using a one-way ANOVA [$F(2, 53) = 0.449$, $p = 0.64$]. Post hoc comparisons using a Tukey HSD test found that there is no significant difference in respiration rate of day 3 male tau flies ($n = 22$) compared to day 10 male tau flies ($n = 19$) ($p = 0.8989538$), no significant difference in respiration rate of day 10 male tau flies compared to day 20 male tau flies ($n = 15$) ($p = 0.6128760$), and no significant difference in respiration rate of day 3 male tau flies compared to day 20 male tau flies ($p = 0.8387658$).

8. Female control flies show upwards respiration trend during aging, female tau flies show downwards respiration trend during aging

After finding significant differences in respiration rate of male and female control flies from day 3 to day 10, a linear regression model was fitted to assess a trendline of how respiratory rate changes across age. For female control flies, this trendline shows an upwards trend across aging (Fig. 19a). For female tau flies, a linear regression model fitted a trendline that shows a downwards trend across aging (Fig. 19b).

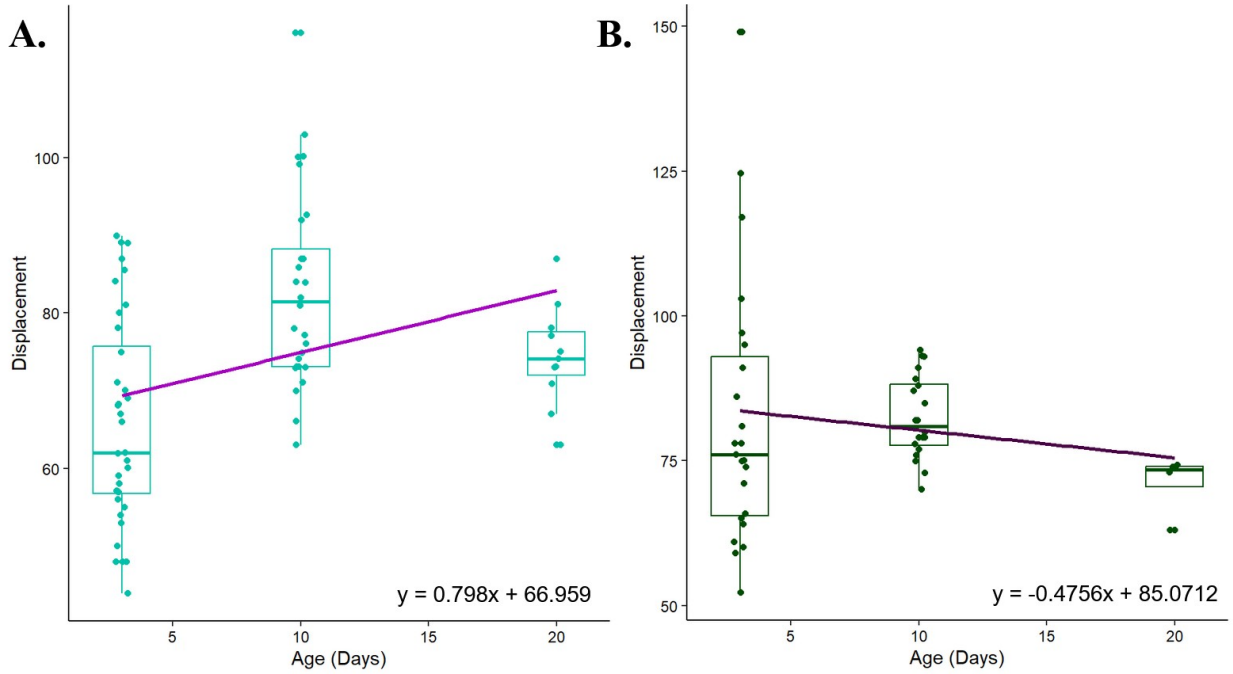

Figure 19. Female control flies show upwards respiration trend during aging, female tau flies show downwards respiration trend during aging. (A) A linear regression line was fitting for the female control data across aging (y = 0.798x + 66.959). This model predicts that as female control flies age, their respiration rate increases. (B) Fitting a linear regression line for female tau data across aging (y = -0.4756x + 85.0712) predicts that as female tau flies age, their respiration rate decreases.

9. Male control flies show upwards respiration trend during aging, male tau flies show downwards respiration trend during aging

After finding significant differences in respiration rate of male and female control flies from day 3 to day 10, a linear regression model was fitted to assess a trendline of how respiratory rate changes across age. For male control flies, this trendline showed a slight upwards trend across aging (Fig. 20a). For male tau flies, a linear regression model fitted a trendline that shows a slight downwards trend across aging (Fig. 20b).

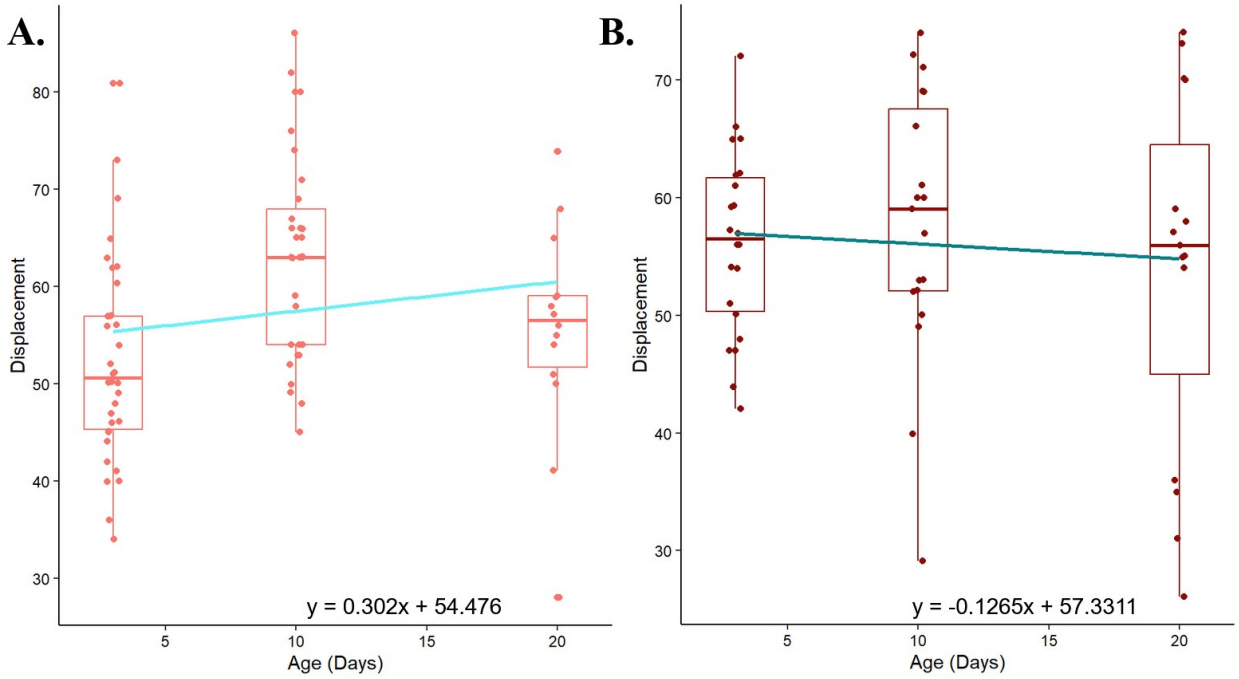

Figure 20. Male control flies show upwards respiration trend during aging, male tau flies show downwards respiration trend during aging. (A) A linear regression line was fitting for the male control data across aging (y = 0.302x + 54.476). This model predicts that as male control flies age, their respiration rate increases. (B) Fitting a linear regression line for male tau data across aging (y = -0.1265x + 57.3311) predicts that as male tau flies age, their respiration rate decreases.

10. Validation of *Drosophila melanogaster* specific antibody to mark γH2Av

10.1 Validation of γH2Av antibody in female control and tau brains

Female flies of both control and tau genetic groups were aged to day 3 or day 20 and immunostained with a *Drosophila* specific primary antibody (MS α his2av) to mark γH2Av, which is found at sites of DSBs (Fig. 21).

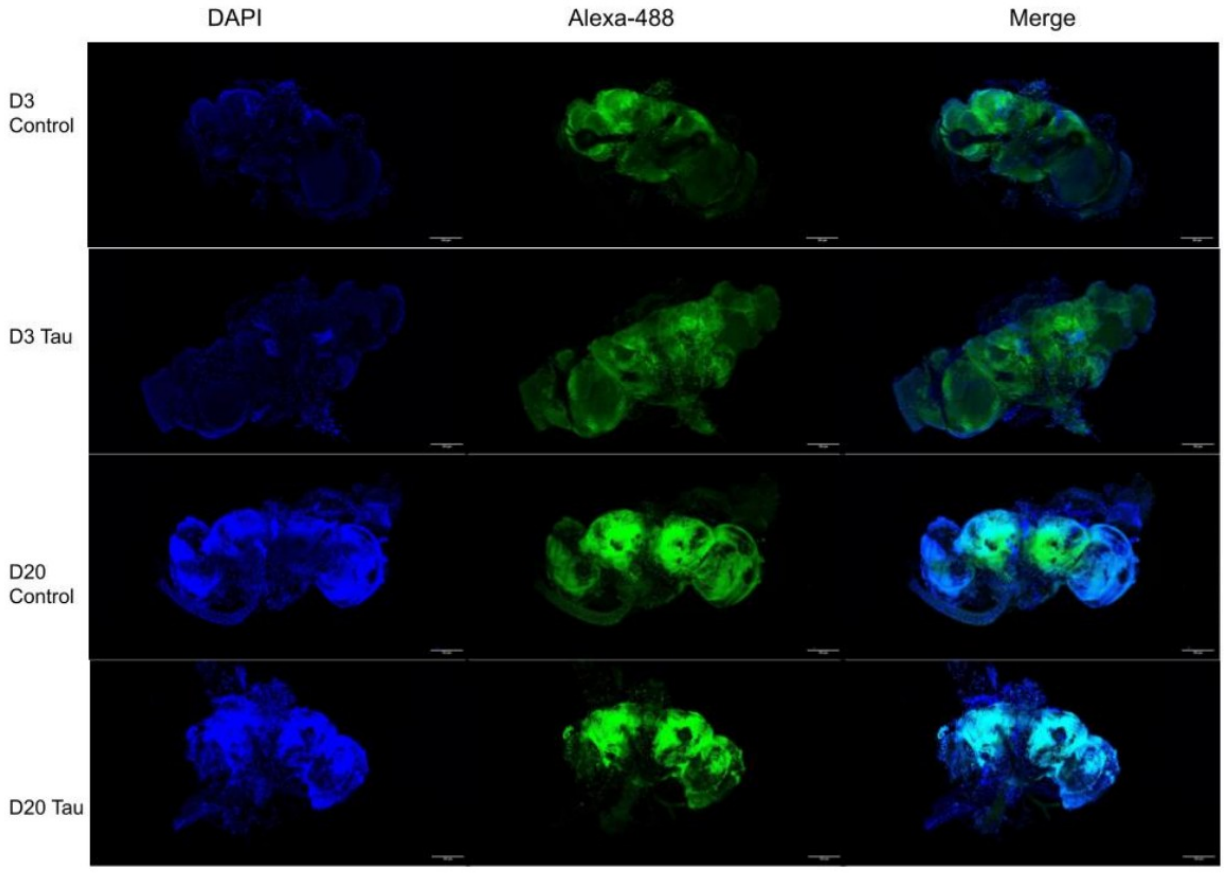

Figure 21. Validation of Drosophila antibody to mark γ-H2AV in female flies. Representative maximum projection Z-stack images of male control and tau flies aged to either day 3 or day 20. Primary immunostaining was done with the *Drosophila* antibody MS α his2av, that marks γ-H2AV. Secondary immunostaining was done with goat-anti mouse Alexa 488 (green). DAPI (blue) was added to the sample prior to mounting. No statistical tests were performed, as this experiment was done to validate a new immunostaining protocol.

10.2 Validation of γH2Av antibody in male control and tau brains

Male flies of both control and tau genetic groups were aged to day 3 or day 20 and immunostained with a *Drosophila* specific primary antibody (MS α his2av) to mark γH2Av, which is found at sites of DSBs (Fig. 22).

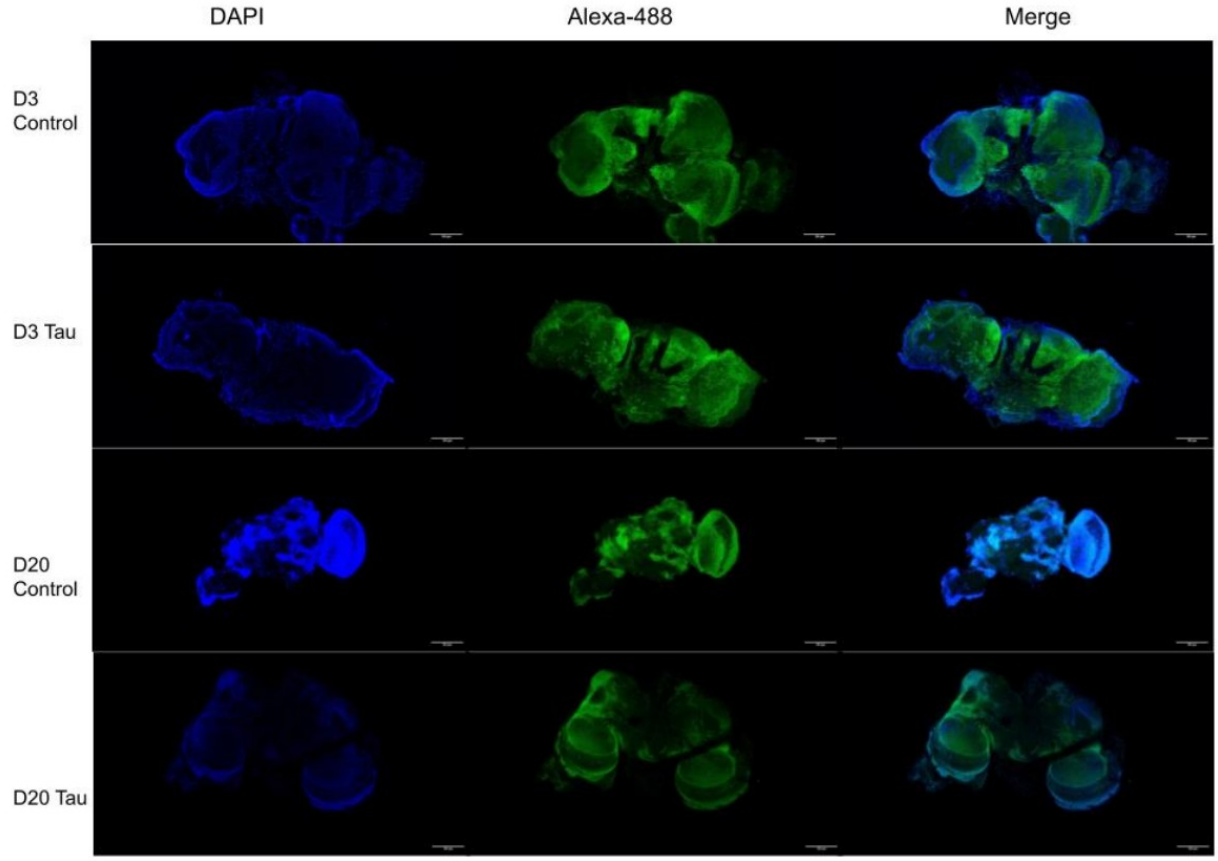

Figure 22. Validation of Drosophila antibody to mark γ-H2AV in male flies. Representative maximum projection Z-stack images of male control and tau flies aged to either day 3 or day 20. Primary immunostaining was done with the *Drosophila* antibody MS α his2av, that marks γ-H2AV. Secondary immunostaining was done with goat-anti mouse Alexa 488 (green). DAPI (blue) was added to the sample prior to mounting. No statistical tests were performed, as this experiment was done to validate a new immunostaining protocol.

DISCUSSION

The quantification of the volumetric respirometry data found a significant difference in respiration rate between males and females across all ages and genotypes. This result led to an importance of male and female as separate categories for future analysis. In control flies of both sexes, there is an increase in respiration from day 3 to day 10, but no difference in respiration rate from day 3 to day 20 or day 10 to day 20. In flies with tau-overexpressing astrocytes of both sexes, there was no difference in respiration rate between day 3 and day 10, day 10 and day 20, or day 3 and day 20. Comparing respiration rates of control flies and tau flies at each age resulted in a sex-specific respiratory pattern. Day 3 female tau flies had a significantly greater respiration rate than day 3 female control flies. This difference was not seen in males at day 3. Fitting linear regression models for each genotype across aging resulted in an upwards trend across aging for control flies, and a downwards trend across aging for tau flies. Additionally, the antibody MS α his2av was validated for staining γH2Av in both sexes.

Respiration rate differs between sexes

Drosophila melanogaster shows an increased respiration rate in females compared to males across all genotypes and ages (Fig. 12). This is likely due to the fact that female flies are larger than male flies. Sex differences in body size, otherwise known as sexual size dimorphism (SSD), is a phenomenon observed across many species of animals including fruit flies. In *Drosophila melanogaster*, female flies on average are about 30% larger than male flies (Sawala & Gould, 2018). As body mass increases, the demand for O_2 also increases. However, oxygen consumption in insects is capped at a maximum value determined by the volume of the tracheal system (Callier & Nijhout, 2011). Limited research is done to determine full body trachea length and volume sex differences, however *Drosophila* intestinal tract researchers have found that female flies have a longer tracheal length, higher number of tracheal branching, and an increased tracheal coverage within gut areas compared to male flies (Blackie et al., 2024). While this is limited to the intestinal tract, this still is evidence that female flies have a larger trachea system and therefore have an increased maximum value of oxygen consumption compared to males.

This supports the results found in this study, as a possible reason for increased female respiration rate is due to an increase in body size and increase in trachea size compared to males.

Future research to further the understanding of sex differences in respiration for *Drosophila* trachea could look into measuring full body trachea length and volume between sexes. One limitation of our study is that no body mass measurements were taken prior to respirometery experiments. Due to this, it is unknown if there was a change in SSD due to genetic manipulations. However, the respirometery data does not suggest that astrocytic tau overexpression alters typical SSD development compared to control. All future research in fruit fly respiration and metabolism should ensure that male and females are separate categories for experimentation and analysis, since females have a higher respiratory rate compared to males.

Respiration rate increases across aging in control flies

Both sexes of the control group were found to have a positively sloped aging-related respiratory trajectory, meaning that respiration rate increases across aging. For both sexes of the control group, respiration rate increases from day 3 to day 10, however there is no increase in respiration rate from day 10 to day 20 or day 3 to day 20 (Fig. 16, 18). Fitting a linear regression model for this data shows an upwards slope in respiration rate across aging for males and females (Fig. 20, 21).

There is limited other data that show what respiration rate looks like across aging in fruit flies. One *Drosophila melanogaster* respiration study used flies of the *Garrboros* wild strain found and that respiration rate slightly decreases across age from day 1 to day 60. The same study also examined the respiration rate of inbred *Garrboros* flies, and found that there is a slight increase in respiration rate from day 1 to day 20, but then a decrease in respiration rate from day 20 to day 60 (F. Lints & Lints, 1968). Use of the *Garrboros* wild type strain is uncommon, with a total of three studies from the same authors that experimented with the strain (F. A. Lints & Lints, 1969, 1971; F. Lints & Lints, 1968). The flies used in the respirometery experiments in this thesis are of the *w*- genetic background, and therefore the differences observed in respiration rate could be attributed to genetic background. However, the lack of information on the *Garrboros* strain makes it difficult to compare and interpret results found in this study. In addition, a lack of studies examining respiration rate of flies over aging makes it difficult to compare or interpret the results we found. Based on our findings that show an aging difference in respiration, a future direction for all metabolic studies is to include age as a variable that impacts metabolic processes.

It is unclear why a day 10 fly has a greater metabolic demand compared to a day 3 fly. Fruit fly life cycle is a term used to describe development from egg to adult, with no differentiation of sub-stages in the adult category (Markow, 2015). So, it is unknown if there are sub-stages of the adult aging process that could alter respiration. One possible reason for an increase in respiration rate in adulthood is the effects of aging could demand more energy for repair mechanisms and cellular reproduction. This theory suggests that the physical process of cellular aging is metabolically taxing for the fruit fly, resulting in an increase in oxygen needed to sustain processes throughout the rest of adulthood. This theory is maintained by the fact that DNA damage is inextricably linked to the aging process (Yousefzadeh et al., 2021). As flies age, it is inevitable that the DNA will be damaged in some way. DNA damage upregulates metabolic processes within cells, as metabolic enzymes are necessary to recruit DNA repair proteins to the site of DSBs (Cucchi et al., 2021; Moretton & Loizou, 2020). This would result in an increase in oxygen needed to maintain cellular function, which is possibly why there is an increase in respiration rate from day 3 to day 10.

Tau overexpression in astrocytes alters aging-related respiratory trajectory

In contrast to the patterns observed in the control group, both sexes in the tau group were found to have a stagnant aging-related respiratory trajectory, meaning that respiration rate did not change across aging. For both sexes of the tau group, respiration rate does not change across any age (Fig. 17, 19). In the control group, there is an increase in respiration rate between day 3 and day 10. However in the tau group, the day 3 respiration rate is equivalently high to the respiration rate at day 10. This result goes against the hypothesis posited for this project, as a decrease in respiration in flies with tau-overexpressing astrocytes was predicted. However, fitting a linear regression model for this data shows a slight downwards slope in respiration rate across aging for males and females (Fig. 20, 21).

One reason why we predicted to see a decrease in respiration rate with age in tau flies is that neurovascular dysfunction is observed in AD pathology (Kisler et al., 2017). To understand more about the link between neurovascular dysfunction and neurodegeneration, a study done in young female mice imaged cerebral vascular reactivity (CVR) in an amyloid beta mouse model of AD, and a tau mouse model of AD (Wells et al., 2015). CVR is a measure of the ability for blood vessels to dilate or constrict in response to a change in arterial CO_2. The results found that

CVR is decreased in the amyloid beta mouse model, but increased in the tau mouse model (Wells et al., 2015). This shows that the neurovascular dysfunction observed in AD is due to amyloid beta deposits, and provides an explanation as to why neurovascular coupling deficits are not seen in primary tauopathies.

The increase in respiration rate at day 3 for female tau flies concur with the results found in Wells *et al*., 2015. This is further evidence to suggest that tau pathology increases the cellular demand for O_2, potentially due to DNA damage resulting in TCA cycle upregulation. Tau toxicity damages DNA indirectly through damaging mitochondria, which results in an increase in ROS that damages DNA. The DNA damage repair response can upregulate the metabolic processes within a cell, resulting in an increase in oxygen consumption needed to fuel cellular processes. If the cell is unable to meet the demand for cellular respiration to repair double-stranded breaks, this results in cellular senescence and apoptosis. This theory suggests that tau pathology expedits the cellular aging process, which is energetically taxing.

Another theory on why there is a significant difference in respiration rate for day 3 tau females, is that astrocyte specific tau-overexpression in fruit flies results in an increase in astrocytes in day 3 female flies, but not in day 3 male flies (Kang, 2023). An increase in the number of astrocytes could increase respiration rate, due to the potential role astrocytes have to modulate the respiratory process within insect brains. Rapidly producing more astrocytes may be a unique, sex-specific adaptation of young female flies with tau pathology to meet the demand for oxygen, similar to the increase in CVR seen in young female mice with tau pathology.

Immunostaining day 3 astrocytic tau-overexpressing female flies for PCNA, showed higher levels of PCNA markers compared to LacZ controls (Kang, 2023). PCNA is essential for DNA replication, and is used as a marker for cell proliferation (Ye et al., 2020). There are several post-translational modifications that PCNA can undergo that change its function within the cell. When ubiquitinated, PCNA becomes a part of the DNA repair process as it is involved in translesion synthesis across damaged DNA (Strzalka & Ziemienowicz, 2011). The antibody used to immunostain PCNA does not differentiate between PCNA and ubiquitinated PCNA, so the increase in PCNA markers in day 3 female flies could be due to an increase in DNA damage from tau aggregates.

In male flies, there is no significant difference in respiration rate at day 3 between tau and control groups (Fig. 14). This is an unusual result for male flies, as it would be expected to see a

significant difference between tau and control at day 3, due to the difference in respiration from day 3 to day 10 in the control flies and no difference in respiration from day 3 to day 10 in tau flies. This could be due to two different reasons, the first of which is that the difference could not be observed due to the result that males respirate significantly less than females. The second reason is that there could be a sex difference in tau toxicity, response to DNA damage, or efficiency of cellular respiration. Further research would need to be done to substantiate any of those claims.

Linear regression models for both sexes predicted a decrease in respiration rate across aging. One limitation of this study is that respiration rate was only collected of flies aged up to day 20. This was due to the difficulties in keeping tau-overexpressing flies alive past day 25. If it was feasible to measure respiration up to day 60, we predict that respiration rates would decrease from day 20 to day 60. The progression of tau toxicity includes mitochondrial dysfunction, which dents the efficiency of cellular respiration. Since metabolic processes are critical for DNA repair, if the cell is unable to produce the energy needed to repair its DNA, then the cell would become senescent, due to the presence of unrepairable DSBs. DSBs can also be repaired by homologous recombination in dividing cells, and repeated abnormal cell cycle activation can result in apoptosis. Future directions for this project include examining if cellular senescence is a component of *Drosophila* glial tauopathy, and the impact cellular senescence and apoptosis might have on respiration rate across aging.

Validation of Drosophila γH2Av antibody

To break ground on the future direction of the involvement of cellular senescence in *Drosophila* glial tauopathy, we used a *Drosophila* specific antibody, MS α his2av, developed by Lake *et al*., 2013 to mark phosphorylated histone 2AV, a histone present at all DSB sites (Madigan et al., 2002). DSBs trigger the permanent activation of the DNA damage repair response and are considered to be a hallmark indicator of cellular senescence (Bielak-Zmijewska et al., 2018).

While γH2Av is found at locations of DSBs, it is also found to colocalize with insulator proteins at the boundaries between adjacent Topologically Associating Domains (TADs) throughout the genome (Simmons et al., 2022). This is why it appears like every cell contains DSBs (Fig. 21, 22), as the antibody marks γH2Av regardless if the histone is colocalized to an

insulator protein or present at a DSB. Using this antibody alone, there theoretically will be an increase in fluorescence across aging if cellular senescence increases with tau overexpression, however it is unclear. Early stage senescent cells show elevated senescence-associated beta-galactosidase (SA-β-gal) activity (Ito & Igaki, 2016). Additional staining for SA-β-gal has been previously used in conjunction with γH2Av (or homolog γH2AX) antibodies to identify senescent cells (Biran et al., 2017). Future work on this project should look into staining for both SA-β-gal and γH2Av to classify senescent cells in *Drosophila*.

The time constraints for this project limited the progression that could be made on this experiment, however, we developed a new procedure for immunostaining in Terasaki well plates and validated that the antibody worked. No statistical analysis has been done, as there are few samples of each age and genotype group. Knowing that this antibody works, future research can repeat the preliminary experiments done in this study and look into what cell types are affected by senescence in *Drosophila* glia tauopathy.

Conclusion and Implications

This study lays a groundwork of evidence to suggest that astrocytes are implicated in respiratory processes within the fruit fly brain, although further investigation is still needed. In this study, we found that there is a sex difference in respiration rate in fruit flies. This informs all future research using *Drosophila melanogaster* to treat sex as a separate and important variable with regards to metabolic processes. Additionally, an increase in respiration rate was seen in both sexes of control flies from day 3 to day 10. This suggests that there may be a component to the process of aging that is energetically taxing. Astrocytic tau overexpression results in increased respiration rates for Day 3 female flies and alters aging related respiratory trajectories for both sexes. This result reaffirms the theory that tau pathology increases the cellular demand for oxygen, possibly due to DNA damage.

There are a number of future directions to be pursued based on the results found in this study. The first of which is examining the role of cellular senescence and DNA damage in *Drosophila* glial tauopathy. This will provide further insight on how tau-toxicity induced DNA damage could affect respiratory processes. This thesis provides a glimmer into how respiration is affected by tauopathies, and sets a path for future research in metabolic studies.

LITERATURE CITED

Albers, D. S., Swerdlow, R. H., Manfredi, G., Gajewski, C., Yang, L., Parker, W. D., & Beal, M. F. (2001). Further evidence for mitochondrial dysfunction in progressive supranuclear palsy. *Experimental Neurology*, *168*(1), 196–198. https://doi.org/10.1006/exnr.2000.7607

Anderson, C. M., & Swanson, R. A. (2000). Astrocyte glutamate transport: review of properties, regulation, and physiological functions. *Glia*, *32*(1), 1–14.

Anoar, S., Woodling, N. S., & Niccoli, T. (2021). Mitochondria Dysfunction in Frontotemporal Dementia/Amyotrophic Lateral Sclerosis: Lessons From Drosophila Models. *Frontiers in Neuroscience*, *15*, 786076. https://doi.org/10.3389/fnins.2021.786076

Arendt T. (2012). Cell cycle activation and aneuploid neurons in Alzheimer's disease. *Molecular neurobiology*, *46*(1), 125–135. https://doi.org/10.1007/s12035-012-8262-0

Arnold, P. K., & Finley, L. W. S. (2023). Regulation and function of the mammalian tricarboxylic acid cycle. *The Journal of biological chemistry*, *299*(2), 102838. https://doi.org/10.1016/j.jbc.2022.102838

Attwell, D., Buchan, A. M., Charpak, S., Lauritzen, M., Macvicar, B. A., & Newman, E. A. (2010). Glial and neuronal control of brain blood flow. *Nature*, *468*(7321), 232–243. https://doi.org/10.1038/nature09613

Barros L. F. (2022). How expensive is the astrocyte?. *Journal of cerebral blood flow and metabolism : official journal of the International Society of Cerebral Blood Flow and Metabolism*, *42*(5), 738–745. https://doi.org/10.1177/0271678X221077343

Bielak-Zmijewska, A., Mosieniak, G., & Sikora, E. (2018). Is DNA damage indispensable for stress-induced senescence? *Mechanisms of Ageing and Development*, *170*, 13–21. https://doi.org/10.1016/j.mad.2017.08.004

Biran, A., Zada, L., Abou Karam, P., Vadai, E., Roitman, L., Ovadya, Y., Porat, Z., & Krizhanovsky, V. (2017). Quantitative identification of senescent cells in aging and disease. *Aging Cell*, *16*(4), 661–671. https://doi.org/10.1111/acel.12592

Blackie, L., Gaspar, P., Mosleh, S., Lushchak, O., Kong, L., Jin, Y., Zielinska, A. P., Cao, B., Mineo, A., Silva, B., Ameku, T., Lim, S. E., Mao, Y., Prieto-Godino, L., Schoborg, T., Varela, M., Mahadevan, L., & Miguel-Aliaga, I. (2024). The sex of organ geometry. *Nature*, *630*(8016), 392–400. https://doi.org/10.1038/s41586-024-07463-4

Bloom G. S. (2014). Amyloid-β and tau: the trigger and bullet in Alzheimer disease pathogenesis. *JAMA neurology*, *71*(4), 505–508. https://doi.org/10.1001/jamaneurol.2013.5847

Botero, V., Stanhope, B. A., Brown, E. B., Grenci, E. C., Boto, T., Park, S. J., King, L. B., Murphy, K. R., Colodner, K. J., Walker, J. A., Keene, A. C., Ja, W. W., & Tomchik, S. M. (2021).

Neurofibromin regulates metabolic rate via neuronal mechanisms in Drosophila. *Nature Communications*, *12*(1), 4285. https://doi.org/10.1038/s41467-021-24505-x

Braskie, M. N., Klunder, A. D., Hayashi, K. M., Protas, H., Kepe, V., Miller, K. J., Huang, S. C., Barrio, J. R., Ercoli, L. M., Siddarth, P., Satyamurthy, N., Liu, J., Toga, A. W., Bookheimer, S. Y., Small, G. W., & Thompson, P. M. (2010). Plaque and tangle imaging and cognition in normal aging and Alzheimer's disease. *Neurobiology of aging*, *31*(10), 1669–1678. https://doi.org/10.1016/j.neurobiolaging.2008.09.012

Brand, A. H., & Perrimon, N. (1993). Targeted gene expression as a means of altering cell fates and generating dominant phenotypes. *Development (Cambridge, England)*, *118*(2), 401–415. https://doi.org/10.1242/dev.118.2.401

Cakir, T., Alsan, S., Saybaşili, H., Akin, A., & Ulgen, K. O. (2007). Reconstruction and flux analysis of coupling between metabolic pathways of astrocytes and neurons: application to cerebral hypoxia. *Theoretical biology & medical modelling*, *4*, 48. https://doi.org/10.1186/1742-4682-4-48

Callier, V., & Nijhout, H. F. (2011). Control of body size by oxygen supply reveals size-dependent and size-independent mechanisms of molting and metamorphosis. *Proceedings of the National Academy of Sciences of the United States of America*, *108*(35), 14664–14669. https://doi.org/10.1073/pnas.1106556108

Chen, J.-H., Hales, C. N., & Ozanne, S. E. (2007). DNA damage, cellular senescence and organismal ageing: Causal or correlative? *Nucleic Acids Research*, *35*(22), 7417–7428. https://doi.org/10.1093/nar/gkm681

Christopherson, K. S., Ullian, E. M., Stokes, C. C., Mullowney, C. E., Hell, J. W., Agah, A., Lawler, J., Mosher, D. F., Bornstein, P., & Barres, B. A. (2005). Thrombospondins are astrocyte-secreted proteins that promote CNS synaptogenesis. *Cell*, *120*(3), 421–433. https://doi.org/10.1016/j.cell.2004.12.020

Colodner, K. J., & Feany, M. B. (2010). Glial fibrillary tangles and JAK/STAT-mediated glial and neuronal cell death in a Drosophila model of glial tauopathy. *The Journal of neuroscience : the official journal of the Society for Neuroscience*, *30*(48), 16102–16113. https://doi.org/10.1523/JNEUROSCI.2491-10.2010

Cucchi, D., Gibson, A., & Martin, S. a. (2021). The emerging relationship between metabolism and DNA repair. *Cell Cycle*, *20*(10), 943–959. https://doi.org/10.1080/15384101.2021.1912889

Dickson D. W. (1999). Neuropathologic differentiation of progressive supranuclear palsy and corticobasal degeneration. *Journal of neurology*, *246 Suppl 2*, II6–II15. https://doi.org/10.1007/BF03161076

Dixit, H., Kumar C, S., Chaudhary, R., Thaker, D., Gadewal, N., & Dasgupta, D. (2021). Role of Phosphorylation and Hyperphosphorylation of Tau in Its Interaction with βα Dimeric Tubulin

Studied from a Bioinformatics Perspective. *Avicenna journal of medical biotechnology*, *13*(1), 24–34. https://doi.org/10.18502/ajmb.v13i1.4579

Ehrlich, A., Schroeder, C. L., Ehrlich, L., & Schroeder, K. A. (2016). *Medical Terminology for Health Professions, Spiral bound Version*. Cengage Learning.

Feany, M. B., & Dickson, D. W. (1995). Widespread cytoskeletal pathology characterizes corticobasal degeneration. *The American journal of pathology*, *146*(6), 1388–1396.

Fields, R. D., & Stevens-Graham, B. (2002). New insights into neuron-glia communication. *Science (New York, N.Y.)*, *298*(5593), 556–562. https://doi.org/10.1126/science.298.5593.556

Freeman, M. R. (2015). Drosophila Central Nervous System Glia. *Cold Spring Harbor Perspectives in Biology*, *7*(11), a020552. https://doi.org/10.1101/cshperspect.a020552

Freeman, M. R., & Doherty, J. (2006). Glial cell biology in Drosophila and vertebrates. *Trends in Neurosciences*, *29*(2), 82–90. https://doi.org/10.1016/j.tins.2005.12.002

Frost, B., Hemberg, M., Lewis, J., & Feany, M. B. (2014). Tau promotes neurodegeneration through global chromatin relaxation. *Nature Neuroscience*, *17*(3), 357–366. https://doi.org/10.1038/nn.3639

Gourine, A. V., Kasymov, V., Marina, N., Tang, F., Figueiredo, M. F., Lane, S., Teschemacher, A. G., Spyer, K. M., Deisseroth, K., & Kasparov, S. (2010). Astrocytes Control Breathing Through pH-dependent Release of ATP. *Science (New York, N.Y.)*, *329*(5991), 571–575. https://doi.org/10.1126/science.1190721

Hanani, M. (2005). Satellite glial cells in sensory ganglia: From form to function. *Brain Research. Brain Research Reviews*, *48*(3), 457–476. https://doi.org/10.1016/j.brainresrev.2004.09.001

Harada, A., Oguchi, K., Okabe, S., Kuno, J., Terada, S., Ohshima, T., Sato-Yoshitake, R., Takei, Y., Noda, T., & Hirokawa, N. (1994). Altered microtubule organization in small-calibre axons of mice lacking tau protein. *Nature*, *369*(6480), 488–491. https://doi.org/10.1038/369488a0

Hartenstein V. (2011). Morphological diversity and development of glia in Drosophila. *Glia*, *59*(9), 1237–1252. https://doi.org/10.1002/glia.21162

Haydon, P. G., & Carmignoto, G. (2006). Astrocyte control of synaptic transmission and neurovascular coupling. *Physiological reviews*, *86*(3), 1009–1031. https://doi.org/10.1152/physrev.00049.2005

Herman, M. A., Aiello, B. R., DeLong, J. D., Garcia-Ruiz, H., González, A. L., Hwang, W., McBeth, C., Stojković, E. A., Trakselis, M. A., & Yakoby, N. (2021). A Unifying Framework for Understanding Biological Structures and Functions Across Levels of Biological Organization. *Integrative and Comparative Biology*, *61*(6), 2038–2047. https://doi.org/10.1093/icb/icab167

Huang, Y., Ng, F. S., & Jackson, F. R. (2015). Comparison of Larval and Adult Drosophila Astrocytes Reveals Stage-Specific Gene Expression Profiles. *G3: Genes|Genomes|Genetics*, *5*(4), 551–558. https://doi.org/10.1534/g3.114.016162

Ionescu-Tucker, A., & Cotman, C. W. (2021). Emerging roles of oxidative stress in brain aging and Alzheimer's disease. *Neurobiology of Aging*, *107*, 86–95. https://doi.org/10.1016/j.neurobiolaging.2021.07.014

Ito, T., & Igaki, T. (2016). Dissecting cellular senescence and SASP in Drosophila. *Inflammation and Regeneration*, *36*, 25. https://doi.org/10.1186/s41232-016-0031-4

Kang, R. S. (2023). Investigating the Effects of Glial Subtype-Specific Tau Expression in Drosophila melanogaster. *Mount Holyoke College Honors Thesis*

Karanjawala, Z. E., & Lieber, M. R. (2004). DNA damage and aging. *Mechanisms of Ageing and Development*, *125*(6), 405–416. https://doi.org/10.1016/j.mad.2004.04.003

Kaur, P., Khera, A., Alajangi, H. K., Sharma, A., Jaiswal, P. K., Singh, G., & Barnwal, R. P. (2023). Role of Tau in Various Tauopathies, Treatment Approaches, and Emerging Role of Nanotechnology in Neurodegenerative Disorders. *Molecular neurobiology*, *60*(3), 1690–1720. https://doi.org/10.1007/s12035-022-03164-z

Khurana, V. (2008). Modeling Tauopathy in the fruit fly Drosophila melanogaster. *Journal of Alzheimer's Disease: JAD*, *15*(4), 541–553. https://doi.org/10.3233/jad-2008-15403

Khurana, V., Lu, Y., Steinhilb, M. L., Oldham, S., Shulman, J. M., & Feany, M. B. (2006). TOR-mediated cell-cycle activation causes neurodegeneration in a Drosophila tauopathy model. *Current Biology: CB*, *16*(3), 230–241. https://doi.org/10.1016/j.cub.2005.12.042

Kisler, K., Nelson, A. R., Montagne, A., & Zlokovic, B. V. (2017). Cerebral blood flow regulation and neurovascular dysfunction in Alzheimer disease. *Nature Reviews. Neuroscience*, *18*(7), 419–434. https://doi.org/10.1038/nrn.2017.48

Klemmensen, M. M., Borrowman, S. H., Pearce, C., Pyles, B., & Chandra, B. (2024). Mitochondrial dysfunction in neurodegenerative disorders. *Neurotherapeutics*, *21*(1), e00292. https://doi.org/10.1016/j.neurot.2023.10.002

Knowles J. R. (1980). Enzyme-catalyzed phosphoryl transfer reactions. *Annual review of biochemistry*, *49*, 877–919. https://doi.org/10.1146/annurev.bi.49.070180.004305

Kovacs, G. G., Ferrer, I., Grinberg, L. T., Alafuzoff, I., Attems, J., Budka, H., Cairns, N. J., Crary, J. F., Duyckaerts, C., Ghetti, B., Halliday, G. M., Ironside, J. W., Love, S., Mackenzie, I. R., Munoz, D. G., Murray, M. E., Nelson, P. T., Takahashi, H., Trojanowski, J. Q., Ansorge, O., … Dickson, D. W. (2016). Aging-related tau astrogliopathy (ARTAG): harmonized evaluation strategy. *Acta neuropathologica*, *131*(1), 87–102. https://doi.org/10.1007/s00401-015-1509-x

Kovacs, G. G., Lukic, M. J., Irwin, D. J., Arzberger, T., Respondek, G., Lee, E. B., Coughlin, D., Giese, A., Grossman, M., Kurz, C., McMillan, C. T., Gelpi, E., Compta, Y., van Swieten, J. C., Laat, L. D., Troakes, C., Al-Sarraj, S., Robinson, J. L., Roeber, S., Xie, S. X., … Höglinger, G. U. (2020). Distribution patterns of tau pathology in progressive supranuclear palsy. *Acta neuropathologica*, *140*(2), 99–119. https://doi.org/10.1007/s00401-020-02158-2

Kramer, P., & Bressan, P. (2018). Our (Mother's) Mitochondria and Our Mind. *Perspectives on Psychological Science*, *13*(1), 88–100. https://doi.org/10.1177/1745691617718356

Kremer, M. C., Jung, C., Batelli, S., Rubin, G. M., & Gaul, U. (2017). The glia of the adult Drosophila nervous system. *Glia*, *65*(4), 606–638. https://doi.org/10.1002/glia.23115

Kril, J. J., Patel, S., Harding, A. J., & Halliday, G. M. (2002). Neuron loss from the hippocampus of Alzheimer's disease exceeds extracellular neurofibrillary tangle formation. *Acta neuropathologica*, *103*(4), 370–376. https://doi.org/10.1007/s00401-001-0477-5

Lehmann F. O. (2001). Matching spiracle opening to metabolic need during flight in Drosophila. *Science (New York, N.Y.)*, *294*(5548), 1926–1929. https://doi.org/10.1126/science.1064821

Lemaître, C., & Soutoglou, E. (2014). Double strand break (DSB) repair in heterochromatin and heterochromatin proteins in DSB repair. *DNA Repair*, *19*, 163–168. https://doi.org/10.1016/j.dnarep.2014.03.015

Lints, F. A., & Lints, C. V. (1969). Respiration in Drosophila—III influence of preimaginal environment on respiration and ageing in *Drosophila melanogaster* hybrids. *Experimental Gerontology*, *4*(2), 81–94. https://doi.org/10.1016/0531-5565(69)90030-8

Lints, F. A., & Lints, C. V. (1971). Influence of preimaginal environment on fecundity and ageing in *Drosophila melanogaster* hybrids—II. Preimaginal temperature. *Experimental Gerontology*, *6*(6), 417–426. https://doi.org/10.1016/0531-5565(71)90021-0

Lints, F., & Lints, C. (1968). Respiration in drosophilaII. Respiration in relation to age by wild, inbred and hybrid drosophila melanogaster imagos. *Experimental Gerontology*, *3*(4), 341–349. https://doi.org/10.1016/0531-5565(68)90047-8

Logan, M. A. (2017). Glial contributions to neuronal health and disease: New insights from Drosophila. *Current Opinion in Neurobiology*, *47*, 162–167. https://doi.org/10.1016/j.conb.2017.10.008

Ma, Z., & Freeman, M. R. (2020). TrpML-mediated astrocyte microdomain Ca^{2+} transients regulate astrocyte-tracheal interactions. *eLife*, *9*, e58952. https://doi.org/10.7554/eLife.58952

Madigan, J. P., Chotkowski, H. L., & Glaser, R. L. (2002). DNA double-strand break-induced phosphorylation of Drosophila histone variant H2Av helps prevent radiation-induced apoptosis. *Nucleic Acids Research*, *30*(17), 3698–3705.

Markow, T. A. (2015). The secret lives of Drosophila flies. *eLife*, *4*, e06793. https://doi.org/10.7554/eLife.06793

Miller, D., Hannon, C., & Ganetzky, B. (2012). A mutation in Drosophila Aldolase causes temperature-sensitive paralysis, shortened lifespan, and neurodegeneration. *Journal of Neurogenetics*, *26*(3–4), 317–327. https://doi.org/10.3109/01677063.2012.706346

Morawska, L., & Buonanno, G. (2021). The physics of particle formation and deposition during breathing. *Nature Reviews. Physics*, *3*(5), 300–301. https://doi.org/10.1038/s42254-021-00307-4

Moretton, A., & Loizou, J. I. (2020). Interplay between Cellular Metabolism and the DNA Damage Response in Cancer. *Cancers*, *12*(8), 2051. https://doi.org/10.3390/cancers12082051

Moussian B. (2010). Recent advances in understanding mechanisms of insect cuticle differentiation. *Insect biochemistry and molecular biology*, *40*(5), 363–375. https://doi.org/10.1016/j.ibmb.2010.03.003

Musi, N., Valentine, J. M., Sickora, K. R., Baeuerle, E., Thompson, C. S., Shen, Q., & Orr, M. E. (2018). Tau protein aggregation is associated with cellular senescence in the brain. *Aging Cell*, *17*(6), e12840. https://doi.org/10.1111/acel.12840

Nayak, D., Roth, T. L., & McGavern, D. B. (2014). Microglia development and function. *Annual Review of Immunology*, *32*, 367–402. https://doi.org/10.1146/annurev-immunol-032713-120240

Oberheim, N. A., Takano, T., Han, X., He, W., Lin, J. H., Wang, F., Xu, Q., Wyatt, J. D., Pilcher, W., Ojemann, J. G., Ransom, B. R., Goldman, S. A., & Nedergaard, M. (2009). Uniquely hominid features of adult human astrocytes. *The Journal of neuroscience : the official journal of the Society for Neuroscience*, *29*(10), 3276–3287. https://doi.org/10.1523/JNEUROSCI.4707-08.2009

Panda, D., Samuel, J. C., Massie, M., Feinstein, S. C., & Wilson, L. (2003). Differential regulation of microtubule dynamics by three- and four-repeat tau: implications for the onset of neurodegenerative disease. *Proceedings of the National Academy of Sciences of the United States of America*, *100*(16), 9548–9553. https://doi.org/10.1073/pnas.1633508100

Pereanu, W., Kumar, A., Jennett, A., Reichert, H., & Hartenstein, V. (2010). Development-based compartmentalization of the Drosophila central brain. *The Journal of comparative neurology*, *518*(15), 2996–3023. https://doi.org/10.1002/cne.22376

Pereanu, W., Spindler, S., Cruz, L., & Hartenstein, V. (2007). Tracheal development in the Drosophila brain is constrained by glial cells. *Developmental biology*, *302*(1), 169–180. https://doi.org/10.1016/j.ydbio.2006.09.022

Pereanu, W., Shy, D., & Hartenstein, V. (2005). Morphogenesis and proliferation of the larval brain glia in Drosophila. *Developmental biology*, *283*(1), 191–203. https://doi.org/10.1016/j.ydbio.2005.04.024

Rose, J., Brian, C., Woods, J., Pappa, A., Panayiotidis, M. I., Powers, R., & Franco, R. (2017). Mitochondrial Dysfunction in Glial Cells: Implications for Neuronal Homeostasis and Survival. *Toxicology*, *391*, 109–115. https://doi.org/10.1016/j.tox.2017.06.011

Rossi, M. J., & Pekkurnaz, G. (2019). Powerhouse of the mind: Mitochondrial plasticity at the synapse. *Current Opinion in Neurobiology*, *57*, 149–155. https://doi.org/10.1016/j.conb.2019.02.001

Salzer, J. L. (2015). Schwann cell myelination. *Cold Spring Harbor Perspectives in Biology*, *7*(8), a020529. https://doi.org/10.1101/cshperspect.a020529

Santello, M., & Volterra, A. (2009). Synaptic modulation by astrocytes via Ca2+-dependent glutamate release. *Neuroscience*, *158*(1), 253–259. https://doi.org/10.1016/j.neuroscience.2008.03.039

Sawala, A., & Gould, A. P. (2018). Sex-lethal in neurons controls female body growth in Drosophila. *Fly*, *12*(2), 133–141. https://doi.org/10.1080/19336934.2018.1502535

Sealey, M. A., Vourkou, E., Cowan, C. M., Bossing, T., Quraishe, S., Grammenoudi, S., Skoulakis, E. M. C., & Mudher, A. (2017). Distinct phenotypes of three-repeat and four-repeat human tau in a transgenic model of tauopathy. *Neurobiology of Disease*, *105*, 74–83. https://doi.org/10.1016/j.nbd.2017.05.003

Selkoe, D. J. (2001). Alzheimer's disease: Genes, proteins, and therapy. *Physiological Reviews*, *81*(2), 741–766. https://doi.org/10.1152/physrev.2001.81.2.741

Sheloukhova, L., & Watanabe, H. (2024). Evolution of glial cells: A non-bilaterian perspective. *Neural Development*, *19*, 10. https://doi.org/10.1186/s13064-024-00184-4

Schulz, K. L., Eckert, A., Rhein, V., Mai, S., Haase, W., Reichert, A. S., Jendrach, M., Müller, W. E., & Leuner, K. (2012). A new link to mitochondrial impairment in tauopathies. *Molecular neurobiology*, *46*(1), 205–216. https://doi.org/10.1007/s12035-012-8308-3

Simmons, J. R., An, R., Amankwaa, B., Zayac, S., Kemp, J., & Labrador, M. (2022). Phosphorylated histone variant γH2Av is associated with chromatin insulators in Drosophila. *PLOS Genetics*, *18*(10), e1010396. https://doi.org/10.1371/journal.pgen.1010396

Stork, T., Bernardos, R., & Freeman, M. R. (2012). Analysis of glial cell development and function in Drosophila. *Cold Spring Harbor Protocols*, *2012*(1), 1–17. https://doi.org/10.1101/pdb.top067587

Stork, T., Sheehan, A., Tasdemir-Yilmaz, O. E., & Freeman, M. R. (2014). Neuron-glia interactions through the Heartless FGF receptor signaling pathway mediate morphogenesis of Drosophila astrocytes. *Neuron*, *83*(2), 388–403. https://doi.org/10.1016/j.neuron.2014.06.026

Strzalka, W., & Ziemienowicz, A. (2011). Proliferating cell nuclear antigen (PCNA): A key

factor in DNA replication and cell cycle regulation. *Annals of Botany*, *107*(7), 1127–1140. https://doi.org/10.1093/aob/mcq243

Tabeshmehr, P., & Eftekharpour, E. (2023). Tau; One Protein, So Many Diseases. *Biology*, *12*(2), 244. https://doi.org/10.3390/biology12020244

Takano, T., Tian, G.-F., Peng, W., Lou, N., Libionka, W., Han, X., & Nedergaard, M. (2006). Astrocyte-mediated control of cerebral blood flow. *Nature Neuroscience*, *9*(2), 260–267. https://doi.org/10.1038/nn1623

Tan, C. X., Burrus Lane, C. J., & Eroglu, C. (2021). Role of astrocytes in synapse formation and maturation. *Current topics in developmental biology*, *142*, 371–407. https://doi.org/10.1016/bs.ctdb.2020.12.010

Trojanowski, J. Q., Schuck, T., Schmidt, M. L., & Lee, V. M. (1989). Distribution of tau proteins in the normal human central and peripheral nervous system. *The journal of histochemistry and cytochemistry : official journal of the Histochemistry Society*, *37*(2), 209–215. https://doi.org/10.1177/37.2.2492045

Valentino, R. R., Tamvaka, N., Heckman, M. G., Johnson, P. W., Soto-Beasley, A. I., Walton, R. L., Koga, S., Uitti, R. J., Wszolek, Z. K., Dickson, D. W., & Ross, O. A. (2020). Associations of mitochondrial genomic variation with corticobasal degeneration, progressive supranuclear palsy, and neuropathological tau measures. *Acta Neuropathologica Communications*, *8*(1), 162. https://doi.org/10.1186/s40478-020-01035-z

Vasile, F., Dossi, E., & Rouach, N. (2017). Human astrocytes: structure and functions in the healthy brain. *Brain structure & function*, *222*(5), 2017–2029. https://doi.org/10.1007/s00429-017-1383-5

Voet, D., Voet, J. G. (2011). Chapter 20: Transport through membranes, Biochemistry (4th ed.) (pp. 760-788). United Kingdom: Wiley.

Volkenhoff, A., Weiler, A., Letzel, M., Stehling, M., Klämbt, C., & Schirmeier, S. (2015). Glial Glycolysis Is Essential for Neuronal Survival in Drosophila. *Cell Metabolism*, *22*(3), 437–447. https://doi.org/10.1016/j.cmet.2015.07.006

Vourkou, E., Paspaliaris, V., Bourouliti, A., Zerva, M.-C., Prifti, E., Papanikolopoulou, K., & Skoulakis, E. M. C. (2022). Differential Effects of Human Tau Isoforms to Neuronal Dysfunction and Toxicity in the Drosophila CNS. *International Journal of Molecular Sciences*, *23*(21), 12985. https://doi.org/10.3390/ijms232112985

Walz W. (2000). Role of astrocytes in the clearance of excess extracellular potassium. *Neurochemistry international*, *36*(4-5), 291–300. https://doi.org/10.1016/s0197-0186(99)00137-0

Wang, W., Zhao, F., Ma, X., Perry, G., & Zhu, X. (2020). Mitochondria dysfunction in the pathogenesis of Alzheimer's disease: Recent advances. *Molecular Neurodegeneration*, *15*(1), 30.

https://doi.org/10.1186/s13024-020-00376-6

Weingarten, M. D., Lockwood, A. H., Hwo, S. Y., & Kirschner, M. W. (1975). A protein factor essential for microtubule assembly. *Proceedings of the National Academy of Sciences of the United States of America*, *72*(5), 1858–1862. https://doi.org/10.1073/pnas.72.5.1858

Wells, J. A., Holmes, H. E., O'Callaghan, J. M., Colgan, N., Ismail, O., Fisher, E. M., Siow, B., Murray, T. K., Schwarz, A. J., O'Neill, M. J., Collins, E. C., & Lythgoe, M. F. (2015). Increased cerebral vascular reactivity in the tau expressing rTg4510 mouse: Evidence against the role of tau pathology to impair vascular health in Alzheimer's disease. *Journal of Cerebral Blood Flow and Metabolism: Official Journal of the International Society of Cerebral Blood Flow and Metabolism*, *35*(3), 359–362. https://doi.org/10.1038/jcbfm.2014.224

Wigglesworth 1939 Wigglesworth, V. B. (1939). Chapter 9: Respiration, The Principles of Insect Physiology (pp. 182-212). United Kingdom: Methuen & Company, Limited.

Yatsenko, A. S., Marrone, A. K., Kucherenko, M. M., & Shcherbata, H. R. (2014). Measurement of metabolic rate in Drosophila using respirometry. *Journal of visualized experiments : JoVE*, (88), e51681. https://doi.org/10.3791/51681

Ye, X., Ling, B., Xu, H., Li, G., Zhao, X., Xu, J., Liu, J., & Liu, L. (2020). Clinical significance of high expression of proliferating cell nuclear antigen in non-small cell lung cancer. *Medicine*, *99*(16), e19755. https://doi.org/10.1097/MD.0000000000019755

Yildirim, K., Petri, J., Kottmeier, R., & Klämbt, C. (2019). Drosophila glia: Few cell types and many conserved functions. *Glia*, *67*(1), 5–26. https://doi.org/10.1002/glia.23459

Yousefzadeh, M., Henpita, C., Vyas, R., Soto-Palma, C., Robbins, P., & Niedernhofer, L. (2021). DNA damage-how and why we age? *eLife*, *10*, e62852. https://doi.org/10.7554/eLife.62852

Zhang, B., Pan, C., Feng, C., Yan, C., Yu, Y., Chen, Z., Guo, C., & Wang, X. (2022). Role of mitochondrial reactive oxygen species in homeostasis regulation. *Redox Report: Communications in Free Radical Research*, *27*(1), 45–52. https://doi.org/10.1080/13510002.2022.2046423

Zonta, M., Angulo, M. C., Gobbo, S., Rosengarten, B., Hossmann, K.-A., Pozzan, T., & Carmignoto, G. (2003). Neuron-to-astrocyte signaling is central to the dynamic control of brain microcirculation. *Nature Neuroscience*, *6*(1), 43–50. https://doi.org/10.1038/nn980

APPENDIX

```
library(rstatix)
library(ggplot2)
library(ggpubr)
library(pwr)
library(EnvStats)
library(dplyr)

#complete respirometery dataset
fulldata <- fulldata %>%
  mutate(Gene = as.factor(Gene)) %>%
  mutate(Age = as.factor(Age)) %>%
  mutate(Sex = as.factor(Sex))

#incomplete respirometery dataset for power analysis
datasample <- datasample %>%
  mutate(Gene = as.factor(Gene)) %>%
  mutate(Age = as.factor(Age)) %>%
  mutate(Sex = as.factor(Sex))

#complete respirometery dataset genotype coded as either control or tau
CombinedControl <- CombinedControl %>%
  mutate(Genotype = as.factor(Genotype)) %>%
```

```
  mutate(Age = as.factor(Age)) %>%
  mutate(Sex = as.factor(Sex))


#power analysis with DataSample (8 or under datapoints per catergory)
model <- aov(Displacement~Gene*Sex*Age, data = datasample)
summary(model)
tukey <- TukeyHSD(model)
results1 <- tukey[["Gene:Sex:Age"]]
output <- eta_squared(model)
output


#Cohen's F = eta sq/ (1-eta sq)
#gene
output[1]/(1-output[1])
#sex
output[2]/(1-output[2])
#Age
output[3]/(1-output[3])




#gene
pwr.anova.test(k=6, f=(output[1]/(1-output[1])), sig.level = 0.05, power= 0.5)
```

```
#sex
pwr.anova.test(k=2, f=(output[2]/(1-output[2])), sig.level = 0.05, power= 0.5)
#age
pwr.anova.test(k=3, f=(output[3]/(1-output[3])), sig.level = 0.05, power= 0.5)

#assessing whether curly had any effect
datasample.2 <- fulldata%>%
  filter(Gene == "UAS-tau x alrm-GAL4 Sp" | Gene == "UAS-tau x alrm-GAL4 CyO")

SpvCyO <- aov(Displacement~Gene*Sex*Age, data = datasample.2)
summary(SpvCyO)
SpvCyOTukey <- TukeyHSD(SpvCyO)
SpvCyOTukey

datasample.3 <- fulldata%>%
  filter(Gene == "alrm-GAL4 x W- Sp" | Gene == "alrm-GAL4 x W- CyO")

SpvCyOControl <- aov(Displacement~Gene*Sex*Age, data = datasample.3)
summary(SpvCyOControl)
SpvCyOTukeyControl <- TukeyHSD(SpvCyOControl)
SpvCyOTukeyControl

#no difference between sp and cy balancers
```

```
#graphs
#sex differences in respiration
sexmodel <- aov(Displacement~Sex, data = CombinedControl)
summary(sexmodel)
sexmodeltukey <- TukeyHSD(sexmodel)
sexmodeltukey


ggboxplot(CombinedControl, x = "Sex", y = "Displacement", color = "Sex", palette =
          c("#00C1AA", "#F8766D"),
          add = "jitter") + stat_n_text()




#combined control vs tau both sexes
CombinedControl <- CombinedControl %>%
  mutate(Genotype = as.factor(Genotype)) %>%
  mutate(Age = as.factor(Age)) %>%
  mutate(Sex = as.factor(Sex))


#Female Combined Control v Tau
FCombinedControl <- CombinedControl%>%
  filter(Sex == "Female")
```

```
FCCTmodel <- aov(Displacement~Genotype*Age, data = FCombinedControl)
summary(FCCTmodel)
FCCTmodeltukey <- TukeyHSD(FCCTmodel)
FCCTmodeltukey
ggboxplot(FCombinedControl, x = "Age", y = "Displacement", color = "Genotype", palette =
          c("#00C1AA", "#004D04"),
          add = "jitter")

#Male Combined Control v Tau
MCombinedControl <- CombinedControl%>%
  filter(Sex == "Male")
MCCTmodel <- aov(Displacement~Genotype*Age, data = MCombinedControl)
summary(MCCTmodel)
MCCTmodeltukey <- TukeyHSD(MCCTmodel)
MCCTmodeltukey
ggboxplot(MCombinedControl, x = "Age", y = "Displacement", color = "Genotype", palette =
          c("#F8766D", "#880F07"),
          add = "jitter")

#Female CC and Tau across age
FTCombinedControl <- FCombinedControl%>%
  filter(Genotype == "Tau")
FTmodel <- aov(Displacement~Age, data = FTCombinedControl)
```

```
summary(FTmodel)
FTmodeltukey <- TukeyHSD(FTmodel)
FTmodeltukey

ggboxplot(FTCombinedControl, x = "Age", y = "Displacement", color = "#004D04",
          add = "jitter")+stat_n_text()

FCCCombinedControl <- FCombinedControl%>%
  filter(Genotype == "Combined Control")
FCmodel <- aov(Displacement~Age, data = FCCCombinedControl)
summary(FCmodel)
FCmodeltukey <- TukeyHSD(FCmodel)
FCmodeltukey

ggboxplot(FCCCombinedControl, x = "Age", y = "Displacement", color = "#00C1AA",
          add = "jitter")+stat_n_text()


#Male CC and Tau across age
MTCombinedControl <- MCombinedControl%>%
  filter(Genotype == "Tau")
MTmodel <- aov(Displacement~Age, data = MTCombinedControl)
summary(MTmodel)
```

```
MTmodeltukey <- TukeyHSD(MTmodel)
MTmodeltukey

ggboxplot(MTCombinedControl, x = "Age", y = "Displacement", color = "#880F07",
          add = "jitter")+stat_n_text()

MCCCombinedControl <- MCombinedControl%>%
  filter(Genotype == "Combined Control")
MCmodel <- aov(Displacement~Age, data = MCCCombinedControl)
summary(MCmodel)
MCmodeltukey <- TukeyHSD(MCmodel)
MCmodeltukey

ggboxplot(MCCCombinedControl, x = "Age", y = "Displacement", color = "#F8766D",
          add = "jitter") + stat_n_text()

#graphs for lines of best fit
FCCCombinedControl.factor<-FCCCombinedControl%>%
  mutate(Age = as.factor(Age))
FemaleControlRegression <- ggplot()+
  geom_boxplot(data = FCCCombinedControl, aes(x=Age, y=Displacement, group = Age), color
          = "#00C1AA")+
  theme(strip.background = element_rect(fill="white"), strip.text.x = element_text(size=14)) +
```

```
        theme(panel.background=element_rect(fill="white")) +
  theme(plot.title = element_text(hjust = 0.5))+
  xlab("Age (Days)") +
  ylab("Displacement")+
  ggtitle("Linear regresion fit for female control accross age") +
  theme(strip.background = element_rect(colour="white"), strip.text.x = element_text(size=16))
        +
  theme(axis.text = element_text(colour = "black"), panel.spacing = unit(1, "lines")) +
  theme(axis.line = element_line(colour = "black")) +
  theme(legend.key = element_rect(fill="white"))+
  theme(strip.placement = "outside")+geom_jitter(data = FCCCombinedControl, aes(x=Age,
        y=Displacement, group = Age), width = 0.25, color = "#00C1AA")+
  geom_smooth(data = FCCCombinedControl, aes(x=Age, y=Displacement), method = "lm", se
        = FALSE, color = "#a700c1")


lm(Displacement~Age, data = FCCCombinedControl)


FemaleTauRegression <- ggplot()+
  geom_boxplot(data = FTCombinedControl, aes(x=Age, y=Displacement, group = Age), color =
        "#004D04")+
  theme(strip.background = element_rect(fill="white"), strip.text.x = element_text(size=14)) +
```

```
        theme(panel.background=element_rect(fill="white")) +
  theme(plot.title = element_text(hjust = 0.5))+
  xlab("Age (Days)") +
  ylab("Displacement")+
  ggtitle("Linear regresion fit for female tau accross age") +
  theme(strip.background = element_rect(colour="white"), strip.text.x = element_text(size=16))
        +
  theme(axis.text = element_text(colour = "black"), panel.spacing = unit(1, "lines")) +
  theme(axis.line = element_line(colour = "black")) +
  theme(legend.key = element_rect(fill="white"))+
  theme(strip.placement = "outside")+geom_jitter(data = FTCombinedControl, aes(x=Age,
        y=Displacement, group = Age), width = 0.25, color = "#004D04")+
  geom_smooth(data = FTCombinedControl, aes(x=Age, y=Displacement), method = "lm", se =
        FALSE, color = "#4d0049")


lm(Displacement~Age, data = FTCombinedControl)


MaleControlRegression <- ggplot()+
  geom_boxplot(data = MCCCombinedControl, aes(x=Age, y=Displacement, group = Age),
        color = "#F8766D")+
  theme(strip.background = element_rect(fill="white"), strip.text.x = element_text(size=14)) +
        theme(panel.background=element_rect(fill="white")) +
```

```
  theme(plot.title = element_text(hjust = 0.5))+
  xlab("Age (Days)") +
  ylab("Displacement")+
  ggtitle("Linear regresion fit for male control accross age") +
  theme(strip.background = element_rect(colour="white"), strip.text.x = element_text(size=16))
        +
  theme(axis.text = element_text(colour = "black"), panel.spacing = unit(1, "lines")) +
  theme(axis.line = element_line(colour = "black")) +
  theme(legend.key = element_rect(fill="white"))+
  theme(strip.placement = "outside")+geom_jitter(data = MCCCombinedControl, aes(x=Age,
        y=Displacement, group = Age), width = 0.25, color = "#F8766D")+
  geom_smooth(data = MCCCombinedControl, aes(x=Age, y=Displacement), method = "lm", se
        = FALSE, color = "#6df1f8")


lm(Displacement~Age, data = MCCCombinedControl)


MaleTauRegression <- ggplot()+
  geom_boxplot(data = MTCombinedControl, aes(x=Age, y=Displacement, group = Age), color
        = "#880F07")+
  theme(strip.background = element_rect(fill="white"), strip.text.x = element_text(size=14)) +
        theme(panel.background=element_rect(fill="white")) +
  theme(plot.title = element_text(hjust = 0.5))+
```

```
  xlab("Age (Days)") +
  ylab("Displacement")+
  ggtitle("Linear regresion fit for male tau accross age") +
  theme(strip.background = element_rect(colour="white"), strip.text.x = element_text(size=16))
        +
  theme(axis.text = element_text(colour = "black"), panel.spacing = unit(1, "lines")) +
  theme(axis.line = element_line(colour = "black")) +
  theme(legend.key = element_rect(fill="white"))+
  theme(strip.placement = "outside")+geom_jitter(data = MTCombinedControl, aes(x=Age,
        y=Displacement, group = Age), width = 0.25, color = "#880F07")+
  geom_smooth(data = MTCombinedControl, aes(x=Age, y=Displacement), method = "lm", se =
        FALSE, color = "#078288")



lm(Displacement~Age, data = MTCombinedControl)


#Parabolic regression
#Female CC and Tau across age


FCCModelpara <- lm(Displacement ~ poly(Age, 2), data = FCCCombinedControl)
FCCModellinear <- lm(Displacement ~ Age, data = FCCCombinedControl)
comparemodels <- anova(FCCModelpara, FCCModellinear)
comparemodels
```

```
AIC(FCCModelpara)

AIC(FCCModellinear)

mean(FCCModelpara$residuals)

mean(FCCModellinear$residuals)

summary(FCCModelpara)

summary(FCCModellinear)
```